Evolution of Isolated Interior Vortices in the Ocean

YVES MOREL

EPSHOM-CMO, Brest, France

JAMES MCWILLIAMS

IGPP, University of California, Los Angeles, Los Angeles, California

(Manuscript received 15 February 1996, in final form 3 October 1996)

ABSTRACT

The beta effect on the evolution of intrathermocline vortices, such as anticyclonic Mediterranean Water eddies (meddies), is investigated in a quasigeostrophic numerical model with fine high vertical resolution.

The authors define two types of structure for isolated vortices depending on the strength of relative vorticity in comparison with vortex stretching. When stretching dominates, the potential vorticity structure consists of poles of opposite sign primarily distributed along the vertical axis. In that case, interactions among the poles can drastically influence the propagation by increasing both the mean speed and its temporal variability. The trajectories are then highly dependent on the initial vertical structure of the vortex. They exhibit loops, cusps, and stagnation phases, and the mean propagation is generally southwestward at a speed of 1–2 cm s^{-1} for an anticyclone. Sometimes a steadily translating structure (modon) emerges and propagates eastward. These modons are persistent (hence stable), and they have a strong axisymmetric component plus a dipolar barotropic component.

1. Introduction

a. Definitions

For vortex dynamics, the potential vorticity (PV) is usually a useful quantity for the analysis of the evolution. In order to avoid confusion between PV, vertical vorticity and horizontal velocity fields, we begin by defining several terms related to them. ''Anticyclone'' or ''cyclone'' will refer to vortices whose vertical vorticity field has the opposite or same sign as the Coriolis frequency and whose horizontal velocity is clockwise or anticlockwise when viewed from above (in the Northern Hemisphere). The ''PV anomaly'' is the signature of the vortex and is defined as the departure of the total PV from the background PV (which is comprised of only the planetary vorticity and ambient density stratification in this paper). Even though it is usually associated with a dominant negative or positive PV anomaly, we will see that an anticyclone or cyclone can have both positive and negative PV anomalies. In the following, a ''pole'' will refer to a well-defined extremum of PV. A ''multipole'' will thus be the generic term for a vortex structure with at least two separated and well-defined PV extrema, and, in particular, a ''dipole'' is a structure with two PV poles of opposite sign. A ''tilted dipole'' is a dipole whose positive and negative poles are located at different depths and are not aligned vertically. Finally, a ''modon'' is a vortex that propagates steadily, that is to say without changing shape, and is distinguished by having a dipolar PV component with a purely horizontal separation.

b. Problem presentation

The North Atlantic circulation has long been associated with the Gulf Stream. Indeed, this current generated by the wind is so strong that it affects the whole basin. However, the hydrography and dynamics of the North Atlantic do not consist only of this intense surface circulation; edging seas pour water of very different characteristics in this basin and play an essential role too. For instance, the Mediterranean Sea feeds the Atlantic with warm and salty water through the Strait of Gibraltar. When they enter the oceanic basin, Mediterranean waters sink to an equilibrium depth of about 1000 m, are flattened against the Iberian continental slope, and later separate to form interior currents (Madelain 1970; Zenk and Armi 1990; Baringer 1993). Recent campaigns at sea have revealed the presence of many anticyclonic interior vortices of Mediterranean origin in the eastern North Atlantic, the meddies. Their formation mechanisms are still somewhat uncertain; both geostrophic adjustment of the gravitationally unstable outflow water and baroclinic instability of the boundary current have been proposed (McWilliams 1985; Prater

Corresponding author address: Dr. Yves Morel, EPSHOM-CMO, B.P. 426, 29275 Brest Cedex, France.
E-mail: morel@shom.fr

1992; Prater and Sanford 1994), but bottom topography and capes could also play important roles (Pichevin and Nof 1995; Chérubin et al. 1995; Baey et al. 1995). Once formed, these meddies wander in the Atlantic for years (Armi et al. 1989; Richardson et al. 1989) and are gradually mixed with the surrounding waters, carrying warm and salty Mediterranean Water over thousands of kilometers. Their general displacement is southwestward at a speed of up to 2 cm s^{-1} (Richardson et al. 1991) but individual trajectories are quite different from one another and exhibit very complicated behaviors with loops, cusps, stagnation periods, and maximum propagation speeds that often reach 5 to 6 cm s^{-1} (Richardson et al. 1989). Many attempts have been made to explain these trajectories as a consequence of the effect of the variation of the Coriolis parameter with latitude (i.e., the ''beta effect'': McWilliams et al. 1986; Beckmann and Käse 1989; Colin de Verdière 1992), but their solutions have generally had smoother and slower propagation than observed. Hogg and Stommel (1990) and Dewar and Meng (1995) have pointed out that the interaction of a meddy with an unsteady large-scale current could also explain the observed sensitivity. It is indeed likely that the large-scale circulation spans at least the upper part of meddies and partly advects them. However, even if advection plays a role in the motion of meddies, this effect may be overestimated in the two-layer models used thus far since they do not resolve the distinct and only weakly overlapping vertical profiles of the background current and the meddy (see Morel 1995b). Also, it seems implausible that some of the complex meddy gyrations are direct reflections of similar gyrations in the large-scale currents.

In this paper we revisit the beta effect on the evolution of submesoscale vortices such as meddies. More precisely we study the dynamics of quasigeostrophic (QG) vortices on the β plane, for which the main vortex signature is localized at mid depth; the velocity profiles and the background stratification (the Brunt–Väisälä frequency) are appropriate for meddies and the eastern North Atlantic.

It is shown that some vortices develop a tendency toward tilting and formation of a nonaxisymmetric multipole, for which the PV poles are not vertically aligned. This structure is often dominated by a tilted dipole with two strong, opposite-sign extrema of potential vorticity located at different depth, as in the idealized heton point-PV configuration (see Hogg and Stommel 1985). This has a strong influence on the propagation, and the trajectories are then very sensitive to the initial vertical structure, reproducing many aspects of the observed trajectories.

We also show that steadily translating vortices, or modons (see Stern 1975), sometimes emerge from our initial configurations. These solutions propagate eastward at a constant speed (1–3 cm s^{-1}) for more than 300 days and preserve their shape. In their two-layer QG numerical solutions, McWilliams and Flierl (1979) described the formation of eastward propagating vortices from axisymmetric initial conditions and associated this behavior with the formation of a transient modon with a strong, superposable, axisymmetric component (a ''rider''). However, their modons are not stable in the sense that their lifetime is rather short. Besides, in their two-layer model, eastward modons seem to emerge only when the initial flows in the two layers are counterrotating. This was analyzed in more detail by Mied and Lindemann (1979) who studied the behavior of a pair of vortices in a two-layer primitive equation model (a cyclone in the lower layer and an anticyclone in the upper layer). They showed that when the orientation of this structure is adequate, it can translate eastward for a long time (150 days) as a modon with a rider.

Flierl et al. (1980) calculated analytical solutions for modons in a two-layer QG model and Berestov (1981) and Kizner (1983) extended this work taking into account a continuous stratification. Their solutions consist of a dipole on which can be superimposed an axisymmetric part of arbitrary amplitude (the rider). Swenson (1987) has tested some of the solutions given in Flierl et al. (1980), and all the modons he tested were numerically unstable as soon as the axisymmetric part was not null. In fact, for an isolated steadily translating structure on the beta plane, the area integral of the barotropic (i.e., depth averaged) component of the streamfunction must be null (Flierl et al. 1983; Flierl 1987), and there must exist counterrotating flow (the azimuthal velocity must change sign). Thus, if the axisymmetric part of the barotropic component is not null, there exists a ring of counterrotating flow surrounding the core of the vortex. As this is often associated with a rather strong horizontal shear, this led to the speculation that such a structure is likely to be unstable and that only strongly ageostrophic axisymmetric modons could persist (Swenson 1987). However, there does not exist any theorem concerning the stability of modons with a strong axisymmetric component.

In a recent paper, Pakyari and Nycander (1995) have given approximate analytical solutions for eastward propagating modons in a two-layer QG model with a baroclinic vertical structure using a perturbation analysis where the basic state is an axisymmetric baroclinic vortex (no barotropic component). But their solutions were not tested for stability in an initial value problem.

To demonstrate that our numerical solutions are steadily translating structures, we will show that the total potential vorticity is a function of the streak function ($\psi + Cy$, where ψ is the streamfunction and C is the propagation speed). Time integration shows that they are stable and their lifetime seems to be limited only by viscous effects.

In the first section, we briefly present the rigid-lid, flat-bottom QG model, then propose a way to classify QG isolated eddies in two main types, depending on their PV structure. The numerical solutions are then

presented in the second section and their trajectories are analyzed and explained. The third section examines modons, and we analyze the spatial structure of the solutions we obtain from our initial anticyclonic vortices. Applications to oceanic vortices such as meddies are discussed in the last section.

2. QG isolated vortices

a. QG model

In this paper, we consider a QG model on the β plane whose inviscid equations rely on the conservation of the total PV. In a baroclinic framework, upper and lower vertical boundary conditions are necessary. For simplicity we make the rigid-lid approximation and consider only the flat-bottom case since we are most interested in interior flows with weak vertical boundary effects. The equations for the conservation of the total PV are then (see Pedlosky 1987)

$$\frac{d}{dt}\Pi = \partial_t\Pi + J(\psi, \Pi) = 0, \tag{1}$$

with the boundary conditions

$$\partial_z\psi = \begin{cases} 0 \text{ at } z = 0 & \text{(2a)} \\ 0 \text{ at } z = -H, & \text{(2b)} \end{cases}$$

where

$$\Pi = \nabla^2\psi + \partial_z(\overline{S}\partial_z\psi) + \beta y \quad \text{is the total PV} \tag{3a}$$

$$\pi = \nabla^2\psi + \partial_z(\overline{S}\partial_z\psi) \quad \text{is the PV anomaly.} \tag{3b}$$

In these equations ψ is the streamfunction, $J(A, B) = \partial_x A\partial_y B - \partial_y A\partial_x B$ is the Jacobian operator, H is the total depth of the fluid (and is a constant here), β is the gradient of the planetary vorticity, and $\overline{S} = f^2/N^2$ is the stratification coefficient (where N is the Brunt–Väisälä frequency).

b. Isolated vortices

In this paper, we will only consider isolated vortices, which we define as vortices associated with an horizontally localized vorticity and streamfunction, whose velocity profile decays faster than $1/r$ ($\|\mathbf{u}\| = o(1/r)$, where r is the distance from the vortex center). Such vortices have zero total circulation (or integral vorticity) in all horizontal planes.

When such a vortex evolves on the β plane, the rate of decrease of its associated streamfunction profile usually becomes less steep and evolves toward $O(1/r)$ (Flierl 1987; Flierl et al. 1983) but it stays isolated [the velocity field decreases as $O(1/r^2)$].

A necessary and sufficient condition for a vortex to be isolated is that the area integral of the relative vorticity ($\zeta = \partial_x v - \partial_y u = \nabla^2\psi$) vanishes at all depths (see for instance Flierl 1987):

$$\int\int \zeta(x, y, z)\, dx\, dy = 0. \tag{4}$$

Although the evidence can be questioned, measurements at sea (Olson 1980) and experiments in big rotating tanks (Morel 1995a) seem to indicate that vortices in nature are often isolated, with a horizontal ring of opposite-sign vertical vorticity surrounding their core.

c. R and S vortices

We now propose a way to classify QG isolated vortices depending on their PV anomaly structure. Here, we only consider vortices with a localized PV anomaly (i.e., for which $\pi \to 0$ far from the center) and a horizontal domain width much bigger than their anomaly size so that it can be considered infinite. Then, in a QG model with a rigid lid and a flat bottom, a necessary and sufficient condition for a vortex to be isolated is that the bulk integral of the PV anomaly is zero:

$$\int\int\int \pi\, dx\, dy\, dz = 0. \tag{5}$$

The PV anomaly is $\pi = \zeta + \eta$ where $\zeta = \nabla^2\psi$ is the vertical relative vorticity and $\eta = \partial_z(\overline{S}\partial_z\psi)$ the stretching term. For an isolated vortex (4) holds and the bulk integral of ζ is then null. The vertical integral of η is always zero and (5) is then straightforward.

Notice that (5) can be rewritten

$$\int\int \zeta_{bt}\, dx\, dy = \int\int \nabla^2\psi_{bt}\, dx\, dy = 0, \tag{6}$$

where ψ_{bt} is the barotropic component of the streamfunction. Equation (6) shows that (4) holds for the barotropic mode, which is thus isolated. Baroclinic modes are associated with a Greens function vanishing at infinity; thus, they are always isolated for a localized PV field. Since it is equivalent to consider modes or depths for Eqs. (1)–(3), this demonstrates that (4) holds at all depths. The previous arguments also underline the fact that only the barotropic component of a vortex can be nonisolated. Thus, if (4) holds at one depth, it holds at all depths when the PV structure is localized.

From (5), we can distinguish two structural patterns for the PV anomalies for an isolated vortex:

- $\zeta \gg \eta$. As the horizontal integral of ζ is null, the main PV anomaly is in this case surrounded by a ring of opposite sign (see Fig. 1a). We will refer to this structure as an ''R-vortex,'' since the way in which (5) is satisfied is dominated by the relative vorticity.
- $\zeta \ll \eta$. As the vertical integral of η is zero, the main PV anomaly is in that case embedded between poles of opposite sign (see Fig. 1b). This pattern will be called an ''S-vortex'' as its PV is dominated by stretching.

It is possible to define a third pattern when $\zeta \approx \eta$, the vortex then having a structure that is mixed R and S, but this kind of structure will not be studied here.

Notice that strong vertical shears in the horizontal

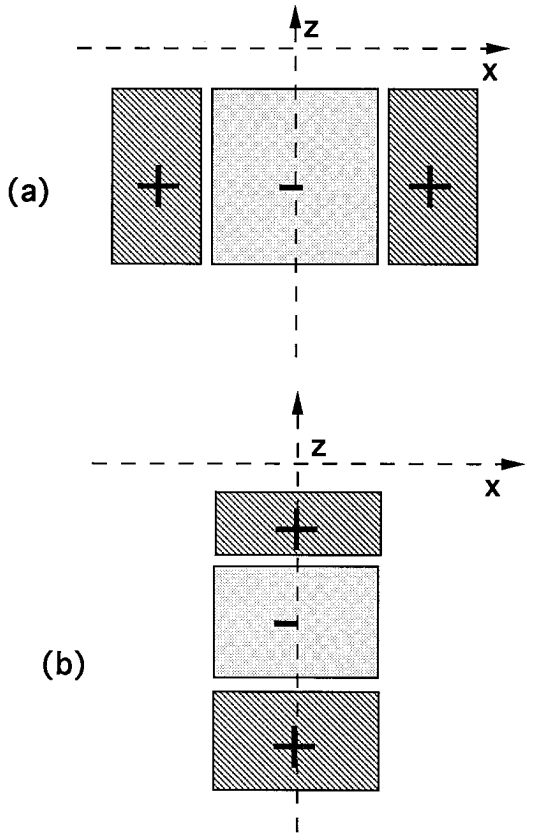

FIG. 1. The two types of PV structures for an isolated vortex. (a) $\zeta > \eta$, R-vortex, the main PV anomaly is surrounded by a ring of opposite sign. (b) $\zeta < \eta$, S-vortex, the main anomaly is embedded between opposite-sign PV poles.

velocity field of a vortex are associated with strong η. Thus, an interior vortex with strong upper and lower vertical shears is an S-vortex.

Most of the previously cited studies of propagation have been for R-vortices, partly as an incidental consequence of choosing sparse vertical resolution. As we shall see, S-vortex propagation can be quite different.

3. Numerical solutions

a. Problem formulation

1) NUMERICAL MODEL

The numerical model we use is a pseudospectral code in the horizontal (a biperiodic domain of width 600 km with a 128 × 128 horizontal grid; Orszag 1971) and a centered second-order finite-difference scheme in the vertical (see McWilliams et al. 1978).

A biharmonic viscosity is used to diminish damping, and the viscosity coefficient of $\nu = 5 \times 10^7$ to 5×10^8 $m^4\ s^{-1}$ is chosen to marginally avoid computational instability. Thus, the viscosity scale ($L_\nu = (\nu/\beta)1/5 \approx 4.8$ km) roughly corresponds to the horizontal grid size ($\Delta x \approx 4.7$ km). The time step is 4320 s, and the model is typically run for 300 days. Usually the vortex does not overlap with the periodic continuation of the Rossby wave wake generated in its propagation within this time period.

To accurately represent the PV structure and evolution, a large number of levels is necessary. We usually use 10 levels for our numerical solutions, which is a major difference with many previous studies on vortex propagation. In addition, our vertical levels are concentrated in regions of high vertical shear through the eddy and depend on the choice of the vertical structure of the vortex (see below). This is done in order to accurately represent the PV anomalies associated with the strong vertical shear at the upper and lower margins of the vortex. This is unconventional as usually levels are chosen so as to accurately represent the vertical structure of the background stratification through the vertical modes (see Beckmann and Kase 1989 or McWilliams et al. 1986). When the vertical resolution is not sufficient, the stretching effect is poorly represented: The dynamical coupling between the levels of strong PV poles is underestimated, and the PV vertical structure of the vortex is smoothed. These biases are particularly important for the evolution of S-vortices.

2) BACKGROUND STRATIFICATION

The background stratification $\bar{\rho}$ is chosen with an exponential decay from the top surface:

$$\bar{\rho} = \rho_o + \Delta\rho(1 - e^{z/H_1}).$$

Notice that z is negative here ($z = 0$ is the free surface and $z = -H = -4000$ m is the bottom). We choose $H_1 = 700$ m in order to have a realistic profile (see, for instance, Armi et al. 1989 or Richardson et al. 1989), and $\Delta\rho = 1.5g/l$ is calculated so that the first internal radius of deformation is 30 km. These choices yield

$$\bar{S} = \frac{f^2}{N^2} = 2.6 \times 10^{-4} e^{-z/700}.$$

3) INITIAL STATE

For S-vortices, we choose the initial structure of the streamfunction as

$$\psi_o = \psi(r, z) = \Psi_o e^{-r^2/R^2} F(z).$$

The vertical structure of the vortex is prescribed as appropriate for a meddy with strong vertical shear above and below the core, as observed in nature (see Armi et al. 1989). Its PV is then dominated by the stretching term whose maximum is 2 to 6 times bigger than the relative vorticity maximum.

For R-vortices, we prescribe the initial PV anomaly as

$$\pi_o = \pi(r, z) = \Pi_o e^{-r^2/R^2}\left(1 - \frac{r^2}{R^2}\right)F(z),$$

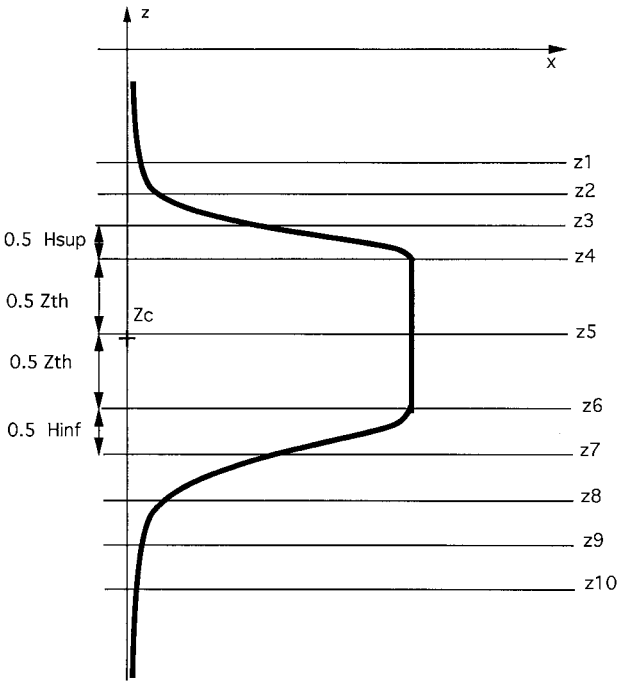

FIG. 2. Description of the vertical grid (10 levels) associated with the initial vertical structure.

where $\Pi_o = -0.6 \times 10^{-4}\ s^{-1}$ and Ψ_o has been chosen so that the maximum relative vorticity $\zeta_{max} = \Psi_o/4R^2 = -0.3 \times 10^{-4}\ s^{-1}$ (an anticyclonic vortex with a turnover time of 5 days).

The vortices associated with each of these formulas are qualitatively similar in their structure. Of course, we could have used a single formula to initialize both types of vortices, using parameter variations to move between the types; however, it was convenient to use these forms, and we do not believe our conclusions are influenced by this procedure.

For both R and S vortices, $R = 30$ km (so that for S-vortices, the maximum velocity is located 22 km from the center of the core). The vertical structure of the vortex $F(z)$ is chosen so as to represent an interior vortex with a core embedded between two vertically sheared regions:

$$F(z) = \begin{cases} e^{-(z-z_1/H_{sup})^2}, & 0 \geqslant z \geqslant z_1 \\ 1, & z_1 \geqslant z \geqslant z_2 \\ e^{-(z-z_2/H_{inf})^2}, & z_2 \geqslant z \geqslant z_{bottom}. \end{cases}$$

The vertical grid we have chosen is a function of z_1, z_2, H_{inf}, and H_{sup} and is illustrated in Fig. 2. By comparison with solutions on finer grids, we have tested that it adequately resolves the vortex evolution.

For each vortex we now define the central depth $Z_c = (z_1 + z_2)/2$ and the thickness $Z_{th} = z_1 - z_2$. Thus, in our experiments we have four parameters relating to vertical structure: the central depth of the vortex Z_c, the vortex thickness Z_{th}, the upper vertical extent H_{sup}, and the lower vertical extent H_{inf}. A wide survey of these parameters was made for each type of vortex, although we concentrated on the parameter ranges associated with observed oceanic vortices (Tables 1 and 2).

TABLE 1. Parameters associated with the vertical structure of R-vortices in Fig. 4a.

Vortex number	Z_c (m)	Z_{th} (m)	H_{sup} (m)	H_{inf} (m)
1	−1000	200	200	200
2	−1000	400	150	150
3	−1000	200	200	400
4	−1100	400	100	100
5	−1100	400	200	200
6	−1100	600	200	400
7	−900	600	200	400

b. Evolution

1) AXISYMMETRIC INSTABILITIES AND MULTIPOLAR EQUILIBRIA

On the f plane (when $\beta = 0$), a necessary condition for a circular vortex to undergo mixed barotropic/baroclinic instabilities is that its radial gradient of PV anomaly changes sign somewhere in the domain (Rayleigh 1880; see also Gent and McWilliams 1986; Flierl 1988). As R or S vortices have PV of both signs, they match this criterion and may be unstable. We have solved the initial value problem on the f plane using our axisymmetric vortices for initial condition and found that they, indeed, often exhibit an unstable tendency. However, for most vortices this instability is weak and does not lead to the breakdown of the initial circular vortex structure into smaller vortices. Instead, the PV rearranges into apparently more stable, nonaxisymmetric, multipolar structures.

Our view is that some form of this process also occurs during a beta-plane evolution, where the stability problem is not cleanly posed because the initial vortex is not a steady solution. However, there it combines with the propagation dynamics, which also contributes to axial asymmetry and tilt among the PV poles.

TABLE 2. Parameters associated with the vertical structure of S-vortices in Figs. 4b and 4c.

Vortex number	Z_c (m)	Z_{th} (m)	H_{sup} (m)	H_{inf} (m)
1	−900	400	400	400
2	−900	400	200	400
3	−900	400	200	300
4	−1100	300	450	300
5	−1100	200	450	300
6	−1100	300	300	300
7	−1100	150	300	300
8	−1100	600	500	400
9	−1100	800	200	600
10	−1100	800	400	400

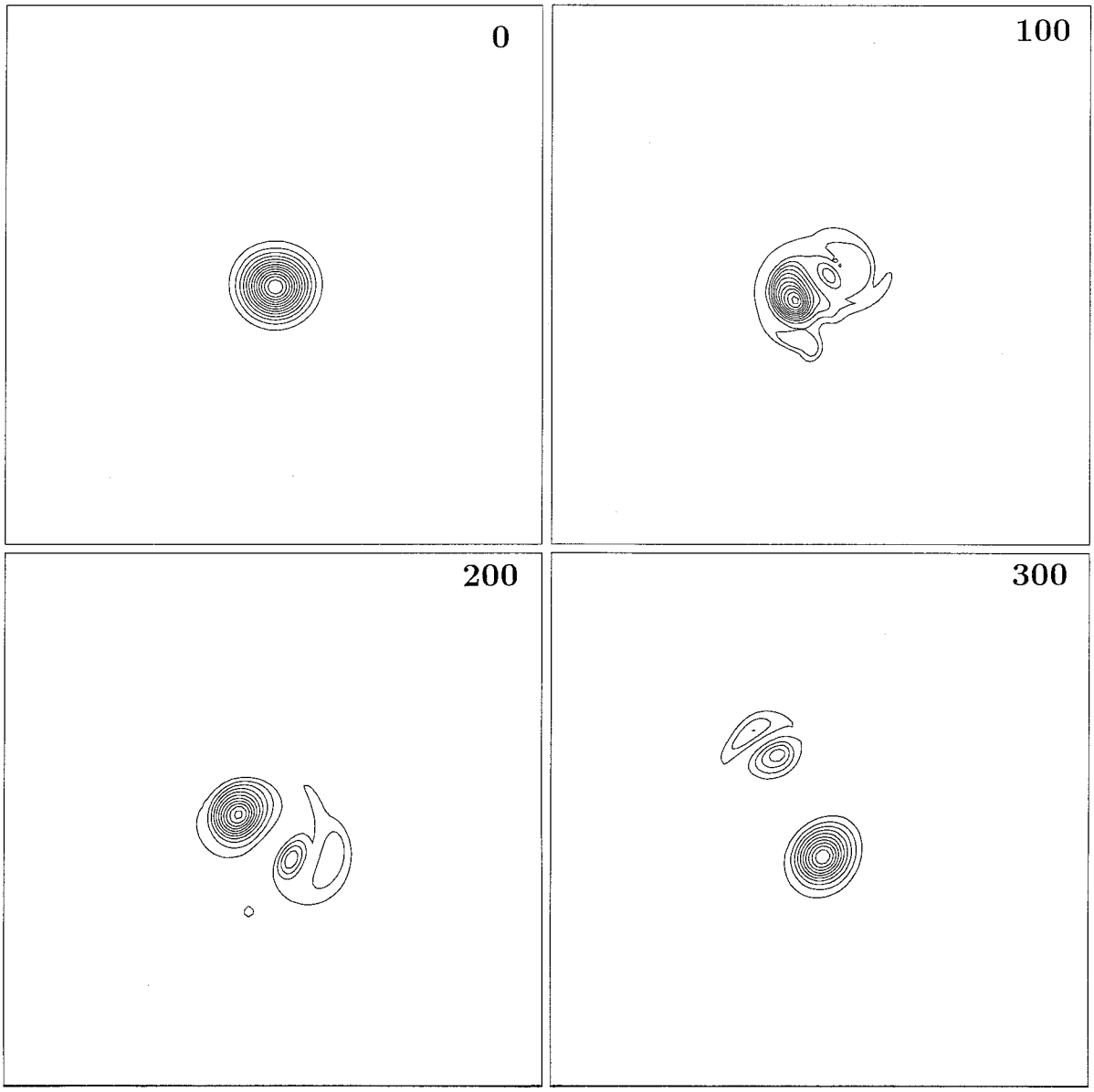

FIG. 3. Evolution of the PV of a S-vortex ($Z_c = -1000$ m, $Z_{th} = 400$ m, $H_{sup} = 200$ m, $H_{inf} = 300$ m) on the f plane at 600 m (a), 1200 m (b), and 1600 m (c). Positive (negative) values of PV are solid (dashed). Times shown are 0, 100, 200, and 300 days.

In a recent paper, Morel and Carton (1994) have studied the stability properties of axisymmetric, barotropic vortices (intrinsically of type R) and the emergence of nonaxisymmetric multipolar equilibria from an unstable circular vortex on the *f* plane. They found that when the number of satellite poles surrounding the main core is more than four, the new multipolar state is unstable too and degenerates. But for up to three satellites, the multipole (dipole, tripole, or quadrapole) can be stable.

Here we find that baroclinic R-vortices are either stable and stay axisymmetric or slightly unstable with the highest growth rate usually for the elliptic mode with azimuthal wavenumber 2. This then leads to the formation of a tripole whose poles are at the same level.

Carton and McWilliams (1989, 1996) have studied the stability of baroclinic axisymmetric vortices and showed that the elliptic azimuthal mode is usually the most unstable. S-vortices are baroclinically unstable, but in our experiments, the first azimuthal mode is unstable too and plays an essential role in the nonlinear evolution. Indeed, S-vortices usually develop a tilt in their vertical axis, which results in a horizontal displacement of the opposite-sign PV poles and again leads to the formation of a tripole, but one whose poles are located at different depths. Because the background stratification varies with depth and the S-vortices are not vertically symmetric initially, this tripolar structure is not symmetric and is often dominated by a dipole. Figure 3 shows the

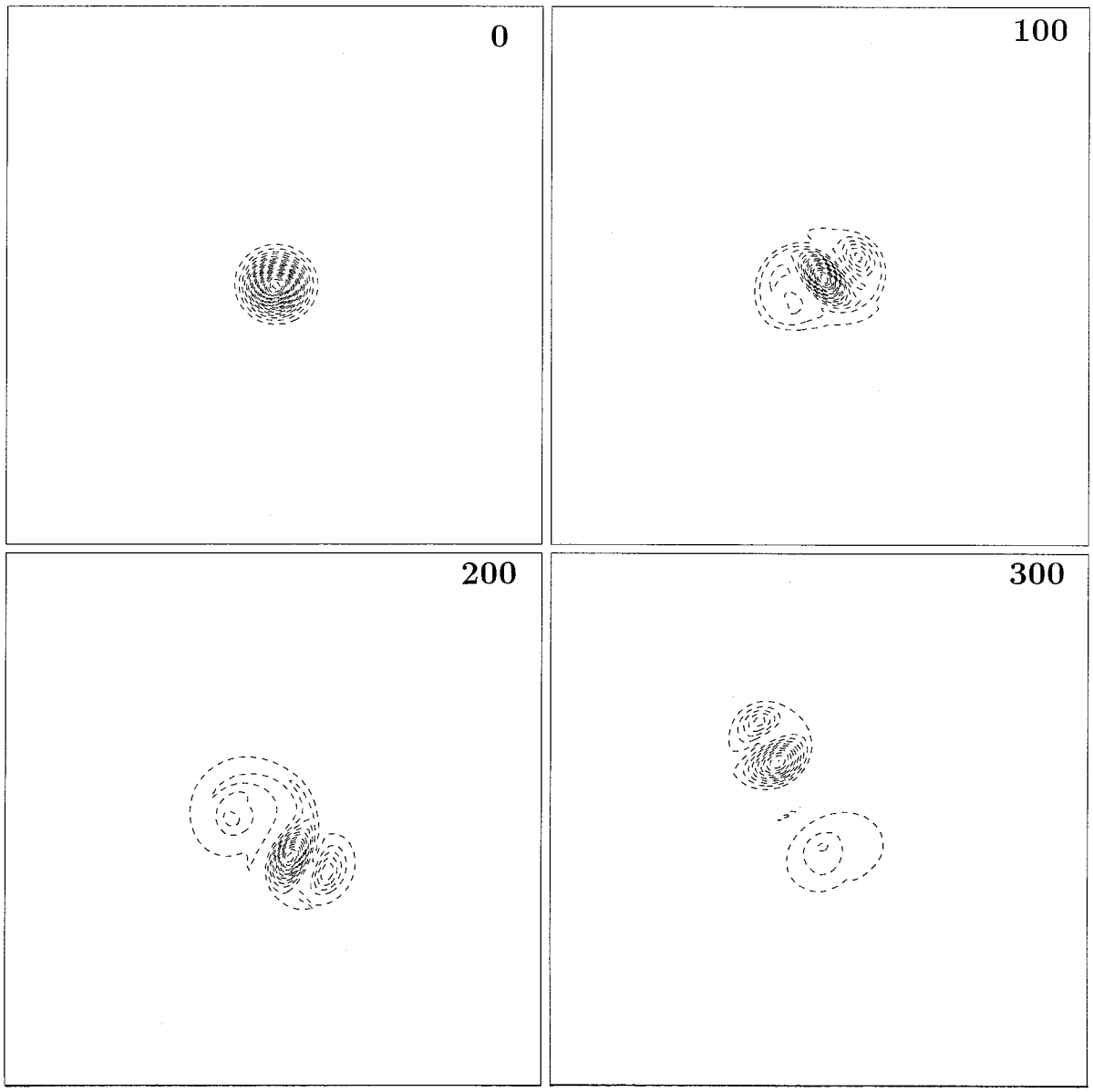

FIG. 3. (*Continued*)

evolution on the f plane of the PV of an S-vortex at three different levels. It is initially dominated by the horizontal displacement of each pole. This leads to the formation of a tilted tripole, with two positive poles rotating anticyclonically above and below the negative core (see Figs. 3a–c at 100 days). As the positive poles usually do not have the same strength, this tripole is not symmetric and its evolution is in general dominated by the interaction between the negative pole and the main positive one. Here, for instance, after 200 days, the upper positive pole has become detached. The evolution is then dominated by the formation of a tilted dipole, which yields a displacement of the vortex core.

For each type of vortex (R or S), time integration shows that the multipolar structures emerging from our initial conditions are essentially stable, in the sense of persisting in their late-time configuration. They are the preferred states for vortices that have PV anomalies of both signs on the f plane (see also Morel and Carton 1994).

Our circular vortices usually have similar initial instability tendencies on the β plane, but the end product of this instability can be different than on the f plane. This strong influence of β on the preferred state is very clear for S-vortices and is probably due to the fact that both β and the highest growth rate act on azimuthal wavenumber one. The result is generally to accelerate the formation of the tilted dipole. It is interesting to

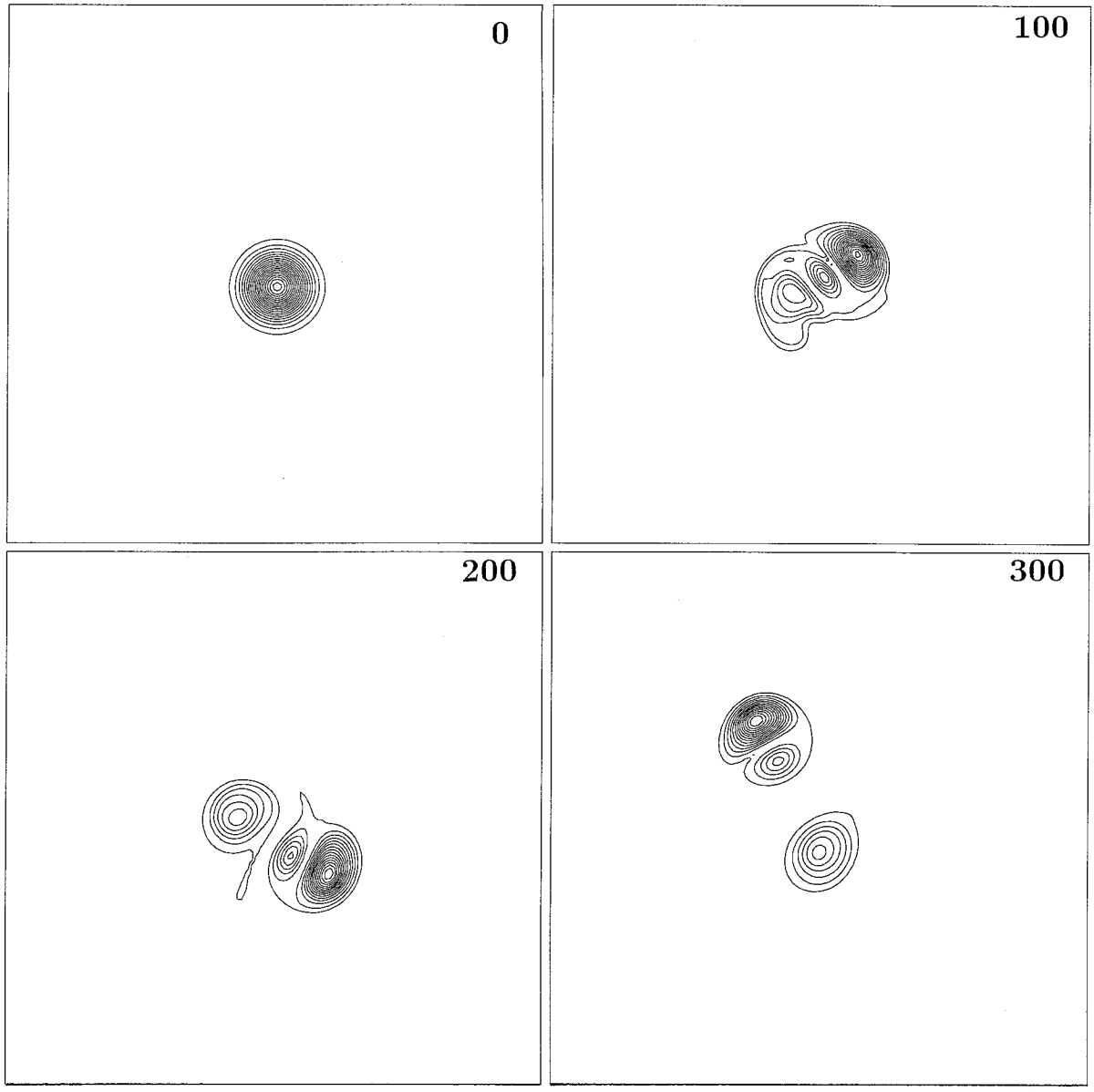

FIG. 3. (*Continued*)

notice that the end product of this initial instability and the trajectory of the vortex was not changed when we superimposed a wavenumber-one perturbation on the axisymmetric vortex. This tends to demonstrate that β plays an important role in determining the result of the instability for S-vortices. So even though R or S vortices are likely to exist only as nonaxisymmetric multipolar states, the results of a previous evolution on an f plane are not satisfactory either for initial conditions. In fact, the choice of the initial state is not crucial for the processes examined in this paper, once a tilted multipole can emerge. We have thus chosen to stick to axisymmetric vortices as they have at least the advantage of giving a clear and precise definition.

Finally, let us mention that the vertical structure of the velocity of the vortex after the unstable stage is not so different from the initial profile, in the sense that strong vertical shears still exist above and below the main anticyclonic core of S-vortices. The principal differences are in the sometimes detached cyclonic partners, whose presence might or might not be detected in sparse field observations.

2) PROPAGATION

Figure 4 shows trajectories for each type of vortex on the β plane. Our solutions for R-vortices do not seem to exhibit very different behavior from one an-

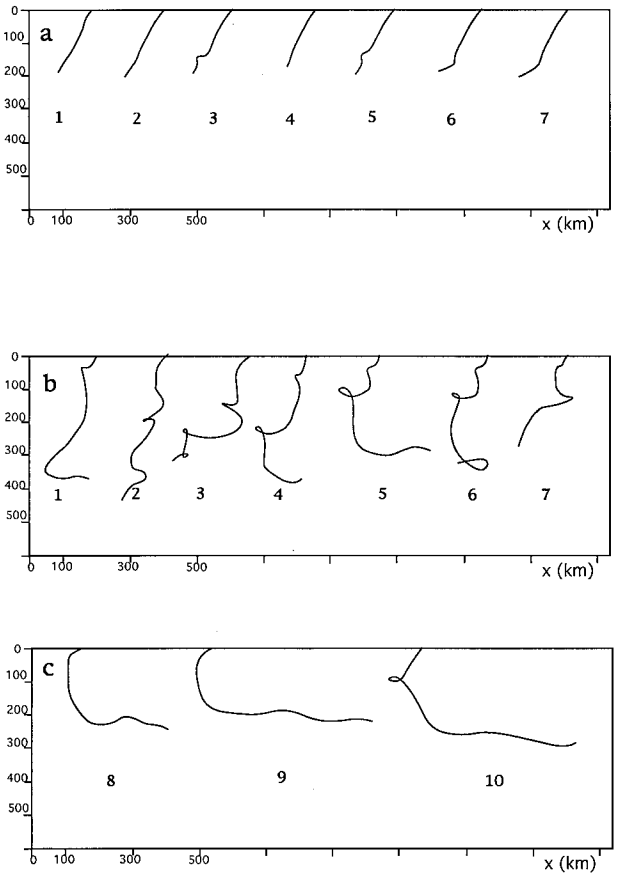

FIG. 4. Trajectories for R-vortices (a) and S-vortices (b) and (c). In the latter case, modons sometimes emerge from the initial anticyclone (c). See Tables 1 and 2 for a description of the parameters of the vortices associated with each trajectory.

other (Fig. 4a; see also Table 1 for a description of the vertical structure of the vortex associated with each trajectory). These trajectories have considerable similarity with what was found in previous studies (see McWilliams and Flierl 1979; McWilliams et al. 1986; Beckmann and Kase 1989): southwestward at an angle of roughly 120° from east; the propagation speed is regular and is less than 1 cm s^{-1}. For S-vortices, the mean displacement is again southwestward, but the paths are often quite complicated, the mean propagation speeds can reach 2 cm s^{-1}, and the instantaneous propagation speeds reach 5 cm s^{-1}. In that case the trajectories exhibit loops, cusps, and stagnation phases (see Fig. 4b and Table 2), as in nature, and sometimes the vortex evolves toward an eastward translating structure (see Fig. 4c and Table 2).

3) INFLUENCE OF THE MULTIPOLE ON THE TRAJECTORY

The effect of β or of any large-scale gradient of background PV on a vortex consists of two parts: advection of the background PV gradient that causes the development of a secondary circulation, called the beta-gyre, and deformation of the initially axisymmetric vortex structure (see McWilliams and Flierl 1979; Sutyrin and Flierl 1994). Both of these effects can induce a displacement. The order of magnitude of the propagation speed due to the β gyre can be estimated taking into account the propagation speed of Rossby waves at the depth of the vortex core $C \approx \beta H^2/\overline{S} \leqslant 1$ cm s^{-1} (with the vortex scale height $H \approx 500$ m, $\beta = 2 \times 10^{-11}$ m^{-1} s^{-1}, and $z = -1000$ m). It has been argued that the development of the beta gyre can give rise to only a limited propagation speed for submesoscale vortices (see McWilliams 1985).

For R-vortices, the result of the initial instability, usually a tripole, has little impact on the displacement of the core in our solutions. At each level, the main core is anticyclonic, and this structure tends to stay vertically aligned. The propagation of R-vortices is thus dominated by the development of the beta gyre, and their trajectories are then regular with a limited displacement speed. However, as entrained particles above and below the main core move southward, they gain positive PV anomalies to conserve total PV, and at later stages even initially R-vortices can become moderate S-vortices and change their behavior. Indeed, we have sometimes noticed that after a lengthy, regular, southward propagation the trajectory of R vortices often changes slightly. Figure 5 shows the trajectory and the evolution of the PV anomaly of an R vortex above the main core. After 200 days, the trajectory changes direction. This could be explained by the formation of a positive PV pole above (or below) the main core (Fig. 5a).

For S-vortices these upper or lower positive PV poles are present and strong since the beginning and induce a quite different behavior. Figures 6a and 6b represent the typical evolution at different depths of the total PV of an S-vortex whose characteristics are $Z_c = -1000$ m, $Z_{\text{th}} = 400$ m, $H_{\text{sup}} = 200$ m, and $H_{\text{inf}} = 300$ m. Figures 6c and 6d represents the evolution of the relative vorticity for the same vortex at the same depths. Each depth corresponds to the main negative (Figs. 6a and 6c) or positive (Figs. 6b and 6d) pole. These two poles are initially aligned, but separate horizontally and evolve so as to form a tilted dipole (Figs. 6a and 6b). As a result of this horizontal separation, a strong cyclonic circulation develops below the core of the vortex whose strength is almost as strong as the main anticyclone (Fig. 6d). Hetonic interactions between opposite-sign PV poles of different strength (Hogg and Stommel 1985) have a major impact on the propagation of the whole structure. The position of the vortex center (extremum of negative PV anomaly) is shown in Fig. 7 and exhibits stagnation points, sudden changes in direction and loops, typical of S-vortices. Figure 8 gives the evolution of the eastward and northward propagation speeds during 300 days for this vortex. These plots have similarities with the plots of observed propagation speeds of meddies (see Fig. 6 of Richardson et al. 1989). Figure 9 represents the tra-

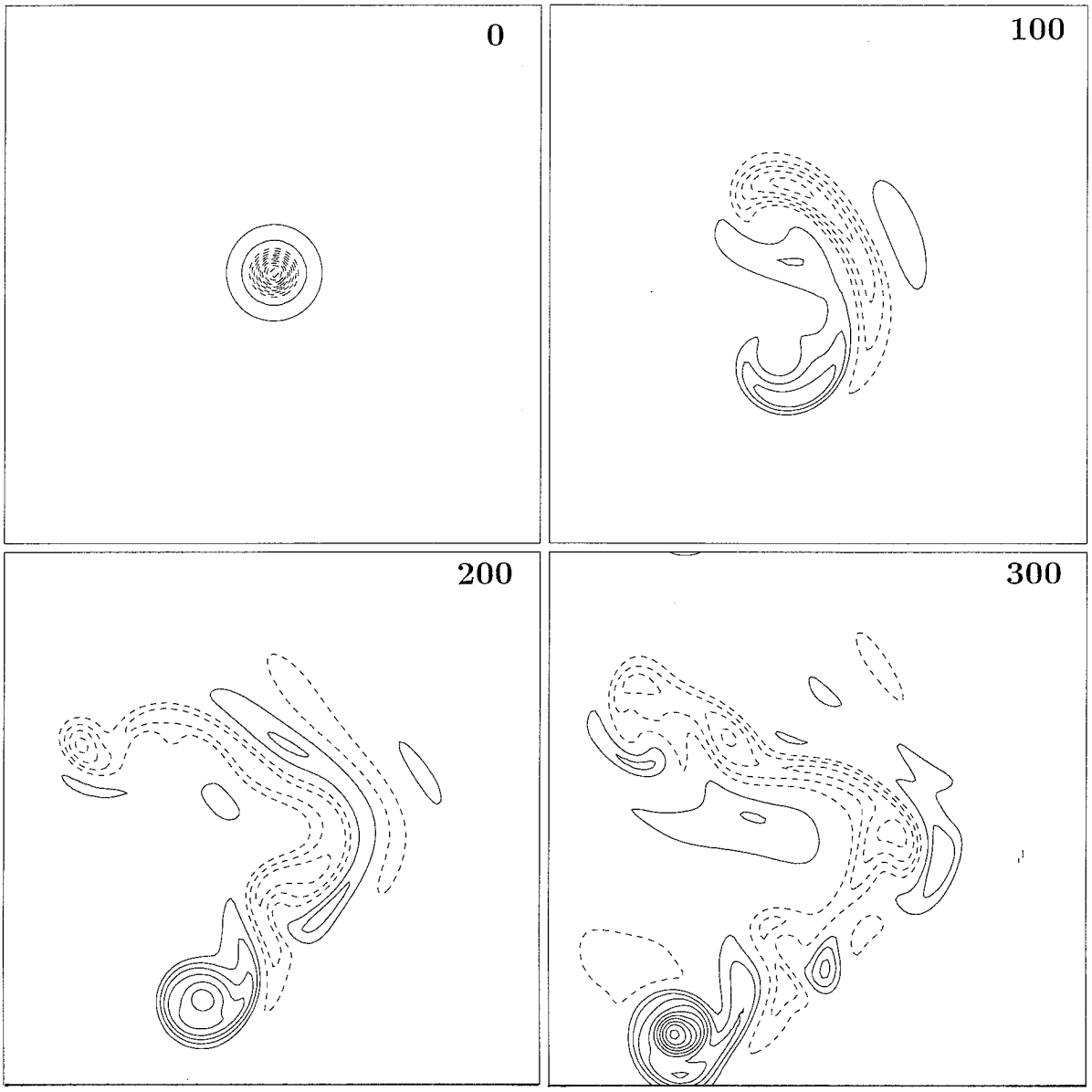

FIG. 5. (a) Evolution of the PV anomaly at a depth of 300 m for an R vortex whose characteristics are $Z_c = -900$ m, $Z_{th} = 600$ m, $H_{sup} = 200$ m, and $H_{inf} = 400$ m (negative PV values are dashed and positive are solid). After 200 days a slight positive PV anomaly develops because fluid particles are displaced southward with the vortex. (b) Trajectory of the center of the vortex; notice the change in direction after 200 days. Times shown are 0, 100, 200, and 300 days.

jectory of the main positive and negative PV poles for the same vortex and put into relief the impact of the dipolar structure on its propagation. There is, indeed, a very good correlation between the direction of propagation of the whole structure and the dipole axis. This is the case for all the S-vortices presented in Figs. 4b and 4c. Thus, both the high propagation speed and its temporal variability are due to the emergence of the tilted dipole, and the observed delicacy of the trajectories is explained by differences in the initial PV structure.

As in our experiments the stratification is weaker and the vortex stretching stronger in the lower part of the vortex, the main cyclonic partner usually emerges below the main core. For different stratification and vortex profiles, however, this cyclonic companion could instead develop above the main vortex core and be evident near the sea surface in temperature or surface elevation.

4) INFLUENCE OF VISCOSITY

It is also clear from Figs. 6a–d that the characteristics (strength and radius) of the PV poles and associated cyclone and anticyclone evolve because of filamentation, dispersion due to Rossby waves, and dissipation.

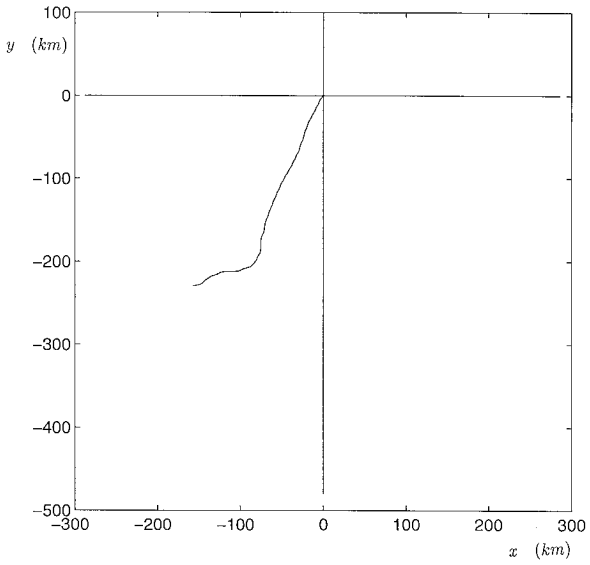

FIG. 5. (*Continued*)

As hetonic interaction depends on the strength and radius of the PV poles, this has an impact on the propagation of the whole structure. The influence of viscosity is particularly clear on the evolution of the maximum total PV, which is only 50%–60% of the initial value after 300 days. The relative vorticity maximum sometimes slightly increases at the beginning when the initially aligned PV poles separate, but after 300 days its strength depends on the vortex structure and ranges from 30% to 60% of the initial value. Viscosity is, of course, a physical property, but in our experiments the magnitude of viscosity has been chosen to ensure numerical stability and the corresponding *e*-folding time is apparently too small in comparison with observations (see Richardson et al. 1989). A few experiments were done to test for the sensitivity of the solutions to viscosity. As long as it stays weak, viscosity has a moderate influence on the behavior of the vortex and only at late stages, after 200 days or so. However, there are a few exceptions as for the same initial conditions but for stronger viscosity (twice the usual one), some solutions evolved toward an eastward instead of southwestward translating structure after 200 days. This shows the sensitivity of the trajectories of S-vortices to details of the dynamical evolution, as well as to initial conditions.

4. Modons

Here we analyze eastward propagating vortices and we shall demonstrate that they are stable modons (i.e., steadily propagating structures), or at least almost such. They have a strong axisymmetric part as well as the characteristic horizontal dipole component. These solutions differ from the previous studies cited in the introduction by arising from interior anticyclones with strong vertical shear.

a. Theory

The best way to demonstrate that these vortices are steadily translating is to construct scatterplots of the total PV against the streak function $\psi + Cy$ where C is the east–west propagation speed. If we suppose that the vortex is steadily translating at a speed $C_x\mathbf{i}$ (where $\mathbf{i}$ is the unit vector along the east–west axis), then $\psi(x, y, z, t) = \psi(x - C_x t, y, z)$ and Eq. (1) can be written in the new coordinate system $X = x - C_x t$, $Y = y$, $Z = z$ (see Stern 1975; Flierl et al. 1980) as

$$-C_x\partial_x\Pi + J(\psi, \Pi) = J(\psi + C_x y, \Pi)$$
$$= J(\psi + C_x y, \pi + \beta y) = 0.$$

Thus, the total PV is an independent functional of the streak function $\psi + C_x y$ at each depth,

$$\pi + \beta y = F(\psi + C_x y, z). \tag{7}$$

Stern (1975) pointed out that the functional $F(\cdot, z)$ needs to be multivalued for a modon solution. For a streak line ($\psi + C_x y = \text{const}$) that extends to infinity, since we are looking for an isolated solution with ψ and π tending toward zero when $r \to \infty$, $F(\cdot, z)$ is fully determined and takes the form $\beta y = F(C_x y, z)$. But for closed streak lines nearer the core of the vortex, $F(\cdot, z)$ can have a different determination. In order to more easily make analytical calculations, Flierl et al. (1980), Berestov (1981), and Kizner (1983) took only linear relationships between the total potential vorticity and the streak function.

b. Analysis of numerical solutions

Figure 10 shows the evolution of the relative vorticity of a vortex whose characteristics are $Z_c = -1100$ m, $Z_{\text{th}} = 800$ m, $H_{\text{sup}} = 200$ m, and $H_{\text{inf}} = 600$ m. After

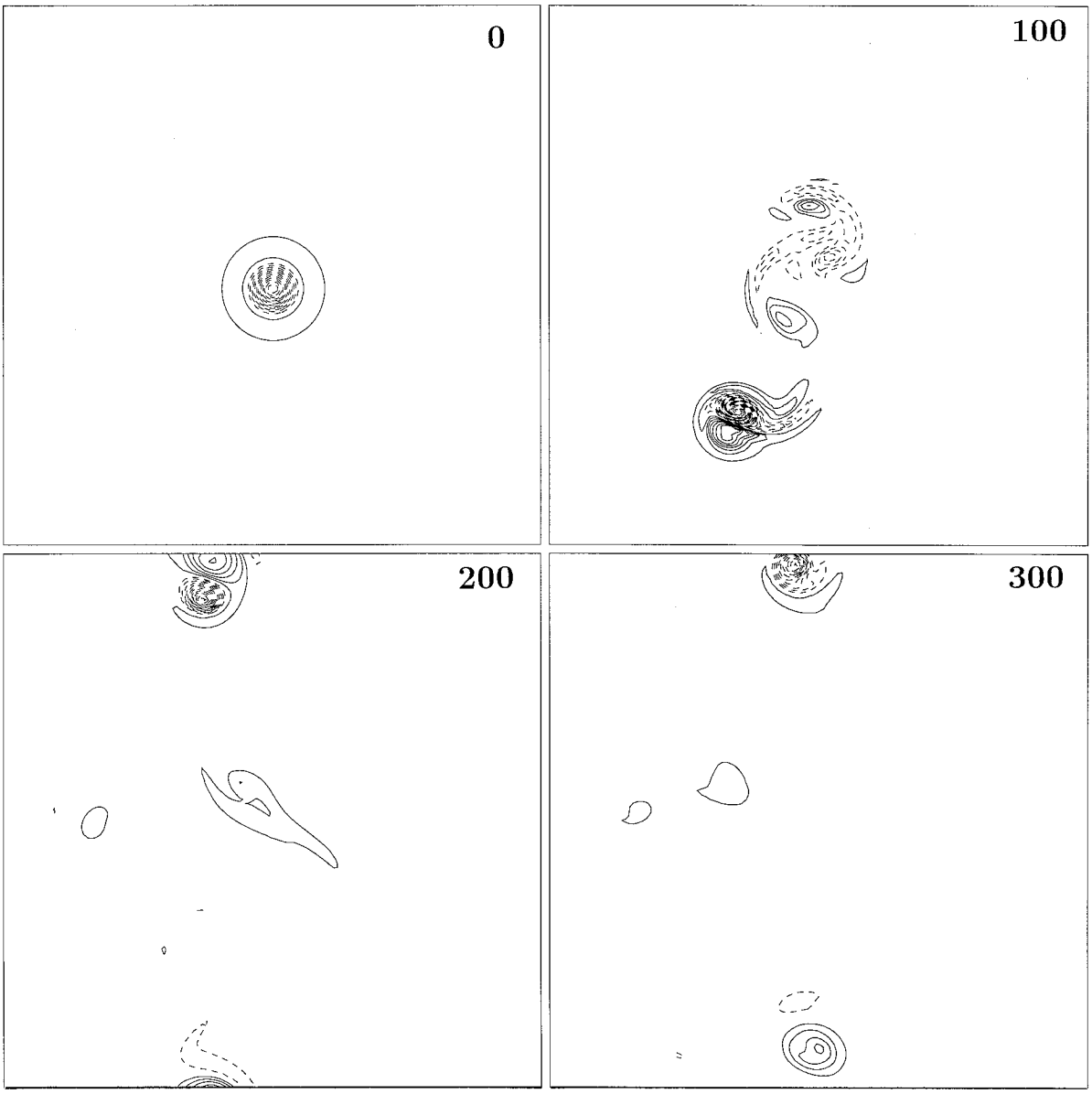

FIG. 6. Evolution every 50 days of the relative vorticity at 1350 m (a) and 1650 m (b) and PV at 1350 m (c) and 1650 m (d) for the S-vortex whose characteristics are $Z_c = -1000$ m, $Z_{th} = 400$ m, $H_{sup} = 200$ m, $H_{inf} = 300$ m (negative values are dashed and positive are solid). A strong cyclonic circulation develops below the core and is associated with the tilting of the structure and the positive PV anomaly. Times shown are 0, 100, 200, and 300 days.

100 days, this vortex propagates eastward and its structure thereafter is persistent. Before analyzing its structure, in order to avoid interaction with residual structures and Rossby waves resulting from the initial rearrangement, the streamfunction of the previous solution at 100 days was filtered (ψ is set to zero beyond a certain radius) and the orientation of the dipole was changed so that it matches the east–west axis. This new structure was then tested numerically as a new initial condition and with a reduced viscosity. When this procedure was repeated for other vortices that exhibited a modon formation tendency, we always ended up with the same results: an increase in the lifetime of the vortex (the eastward propagation and the vortex shape preservation last for more than 300 days) and better scatterplots. Since it is improved when the viscosity is reduced (and the outer field filtered), we think that the lifetime of this structure is limited only by the effect of the viscosity.

Scatterplot of the total PV against the streak function (Q/Ψ plots) can be constructed either by fitting a ''best choice'' for the propagation speed or taking the ob-

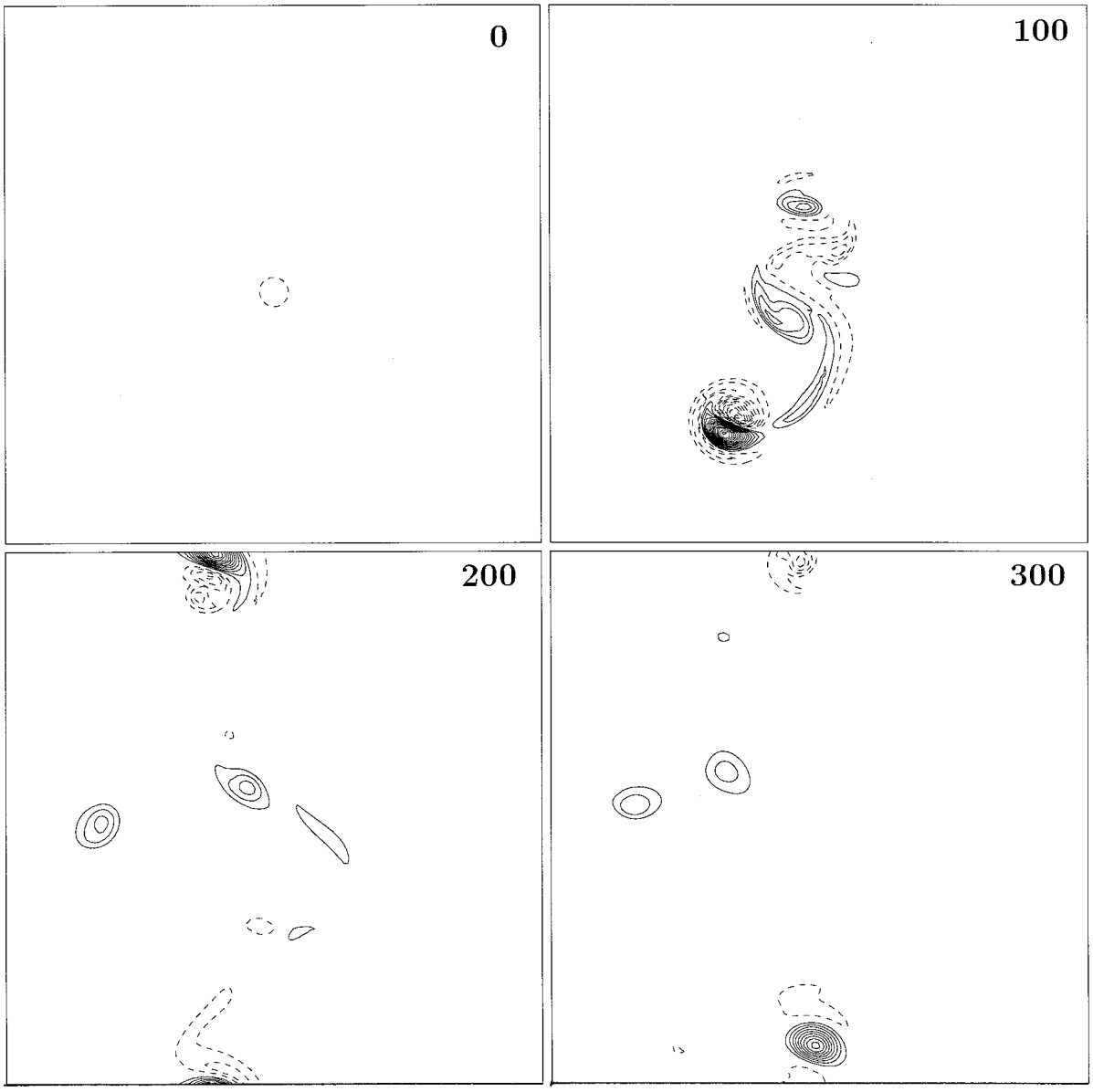

FIG. 6. (*Continued*)

served propagation speed calculated from the plot of the position of the vortex center against time. It is worth noting that the two propagation speeds are very close (the difference is usually less than 5%–10%). The best choice for C_x is the speed that minimizes the scatter about a stationary state

$$S_c = \min_{(C_x,C_y)}\left[\iint_\Omega (J(\psi + C_x y - C_y x,\ \pi + \beta y))^2\ dx\ dy\right]. \quad (8)$$

The domain of integration Ω was usually not the whole domain (although there were no substantial differences, at least at levels where the PV anomaly was significant) because we had the best accordance between the observed propagation speed and the calculated one in each layer when we restricted our area integral to the core of the vortex. This is thought to be the consequence of the remaining Rossby waves due to continuing adjustments of the vortex towards a modon state.

Figure 11 shows the evolution of the scatterplot at a given level for different times. The scatter is reduced during the evolution, and the tendency toward the formation of a modon is clear. Indeed, S_c drastically decreases with time as after 100 days its value is only 10% of the initial one and after 300 days only 1%. In

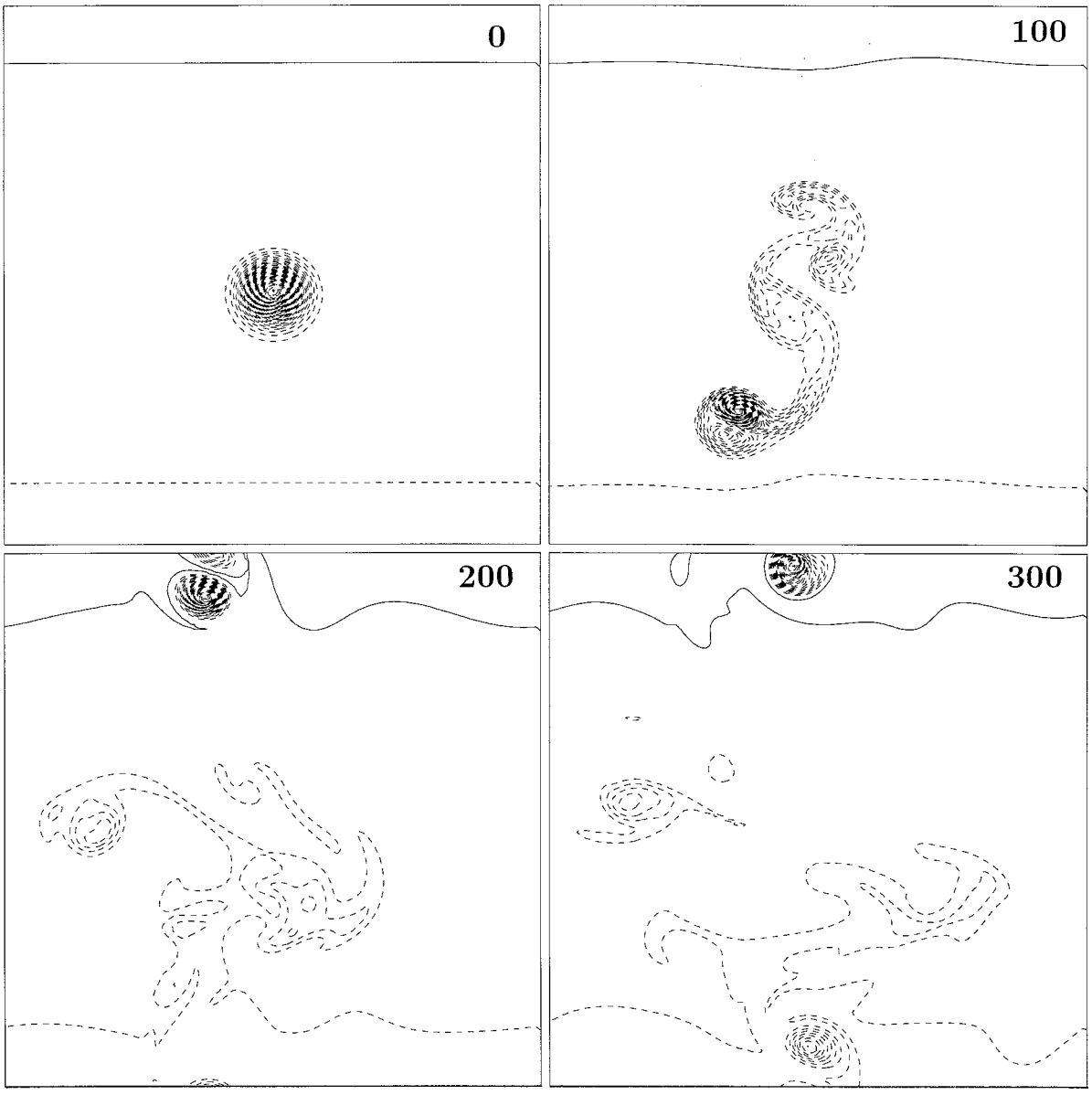

FIG. 6. (*Continued*)

addition, as can be seen from Fig. 10, for instance, these modons have a strong axisymmetric part. The scatterplots in the exterior field are not as good because of Rossby waves that develop initially when the structure is not adjusted. We have filtered out all the remaining traces of Rossby waves from Fig. 11c for the sake of legibility. The exterior region corresponds to the linear Q/Ψ relationship and the interior one to the nonlinear one. The boundary between both regions is the point where the curves match. Notice that, in addition with the exterior region, two different closed streak-line regions can be distinguished. They are associated with the cyclonic and anticyclonic vortices whose signatures are visible at this level and each one has its own determination for F in (7). This is what we can deduce from Fig. 11c, where apparently there are two different Q/Ψ relationships in the closed streakline region of this modon at the same level.

In Fig. 12, we have plotted some scatterplots associated with the previous modon after 300 days of eastward propagation. Since again the remaining traces of Rossby waves outside the vortex spoils the legibility of the plots (especially in the layers near the surface where the PV is weak), we have only included the interior region here. The scatter is weak, which shows that this structure is at least an almost steadily propagating structure on the beta plane. The Q/Ψ relationships in the vortex core are nonlinear, and that transition between

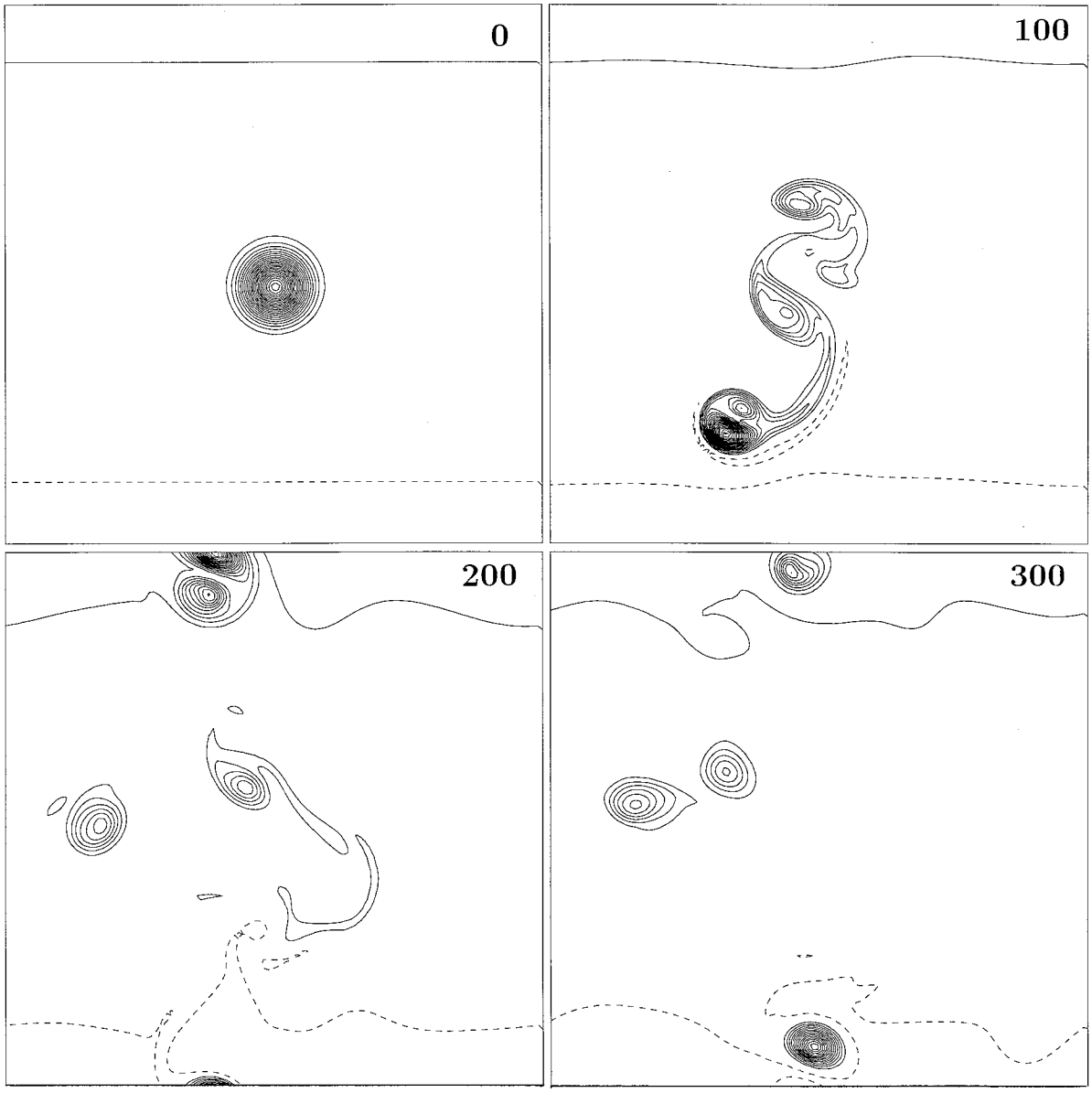

FIG. 6. (*Continued*)

interior and exterior regions seems smooth here (see Fig. 11c).

We show a vertical cross section (north–south) of the total PV field and streamfunction in Fig. 13. The fields have been linearly interpolated vertically and considered constant above $z = -400$ m and below $z = -2700$ m, respectively first and last levels in this numerical solution. Thus, the cyclone (negative values for the streamfunction and positive values for the PV in Fig. 13) extends to the bottom. The structure in PV resembles two symmetric hetons, a strong one and a weak one. The horizontal separation between the center of both main PV poles reaches 60 km, that is to say about twice a vortex radius.

Analytical solutions in a QG model have always relied on linear relationships, which yields to a discontinuity in the radial profile of the PV of the rider (see Flierl et al. 1980). A nonlinear Q/Ψ relationship can generate more nearly continuous PV fields for modon solutions. This in turn is more accurately resolvable in numerical models, which may be at least part of the reason why these solutions are steadier and more stable than those reported earlier.

In an isolated modon on the β plane, the barotropic component of the streamfunction must change sign and satisfies the following integral constraint (Flierl et al. 1983; Flierl 1987):

$$\int\int \psi_{bt}\, dx\, dy = 0. \tag{9}$$

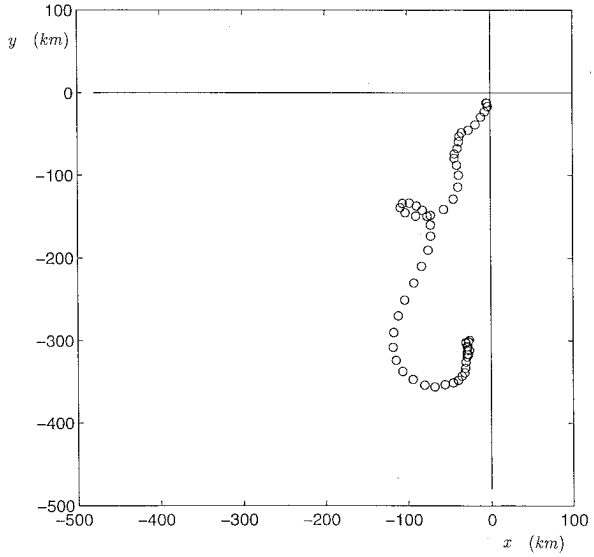

FIG. 7. Position of the center (maximum negative PV anomaly) of the vortex described in Fig. 6. Positions are given every 5 days and for 300 days.

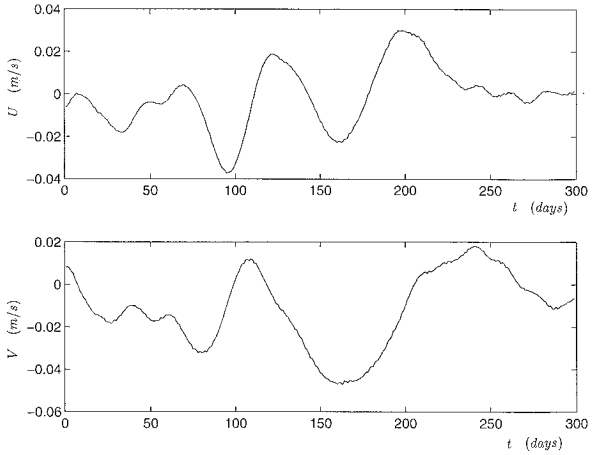

FIG. 8. Eastward (a) and northward (b) propagation speed associated with the vortex described in Fig. 6 and for 300 days of simulation.

Figure 14 represents the barotropic component of the streamfunction associated with the modon studied previously. It is symmetric with respect to the east–west axis and its axisymmetric part is zero or very weak. So, as required, (9) is satisfied. Unlike the Berestov (1981) or Kizner (1983) solutions, which consist of a dipolar barotropic component and an axisymmetric baroclinic rider, the baroclinic part of the modon presented here is not axisymmetric, as the anticyclone and cyclone below are also strongly horizontally separated.

5. Conclusions

a. Summary

We have presented numerical experiments for the evolution of isolated interior QG vortices on the beta plane, for which the bulk integral of the PV anomaly is zero. We have distinguished and analyzed the evolution of two types of vortices depending on the strength of the relative vorticity in comparison with stretching. When the relative vorticity dominates (R-vortices), the PV anomaly structure consists of a main core surrounded by an opposite-sign ring. For these vortices, the propagation is dominated by the development of the β gyre and does not change very much from a vortex to another, at least for our solutions. For meddy parameters the mean propagation speed is then usually less than 1 cm s^{-1} and the trajectory is southwestward and rather regular.

When the vertical shear of the initial current is strong, the stretching dominates and the PV anomaly pattern consist of poles of opposite sign vertically distributed (S-vortices). This structure typically evolves into a nonaxisymmetric multipole often dominated by a tilted dipole. This induces some effects on the displacement of the vortex because of hetonic interactions between the main $\pm$PV poles. The propagation speed can then be drastically enhanced and reach 5 cm s^{-1} for a mean displacement of 1–2 cm s^{-1} southwestward. The details of the path are very sensitive to the initial structure and the trajectories exhibit loops, cusps, and stagnation phases as in nature.

Anticyclonic S-vortices can evolve toward a stable eastward propagating modon with a strong axisymmetric part as rider. The Q/ψ relationships are very nonlinear in the core of the modon and their barotropic components consist of a dipolar structure with little or

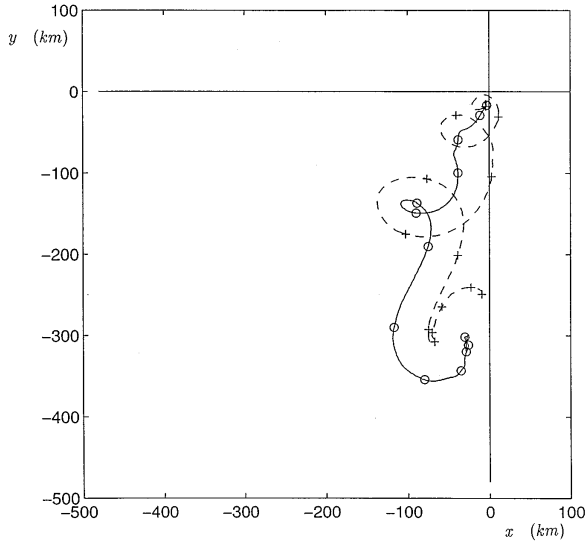

FIG. 9. Trajectory of the main positive (dashed) and negative (plain) PV poles of the vortex in Fig. 6. We have also represented the position of the poles every 25 days (+ for the positive pole and o for the negative one). The direction of propagation of the vortex is given by the axis of the dipole.

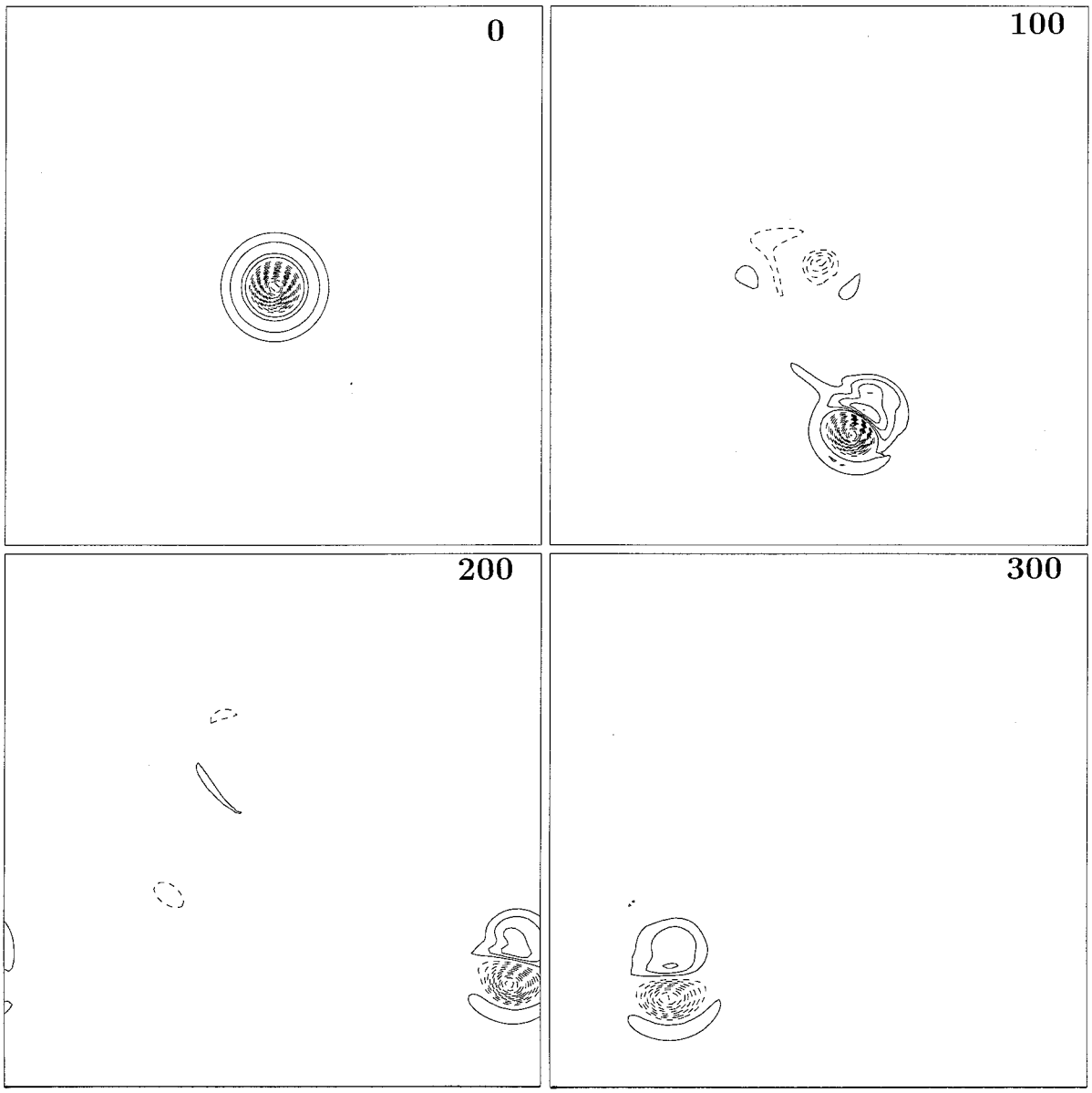

FIG. 10. Evolution of the relative vorticity at the level of the center of a vortex whose initial characteristics are: $Z_c = -1100$ m, $Z_{th} = 800$ m, $H_{sup} = 200$ m, and $H_{inf} = 600$ m (negative values are dashed and positive are solid). A modon is formed after 100 days of evolution. Times shown are 0, 100, 200, and 300 days.

no axisymmetric part. The lifetime seems to be limited only by viscosity.

b. Discussion

Let us first mention that we also perform scatterplots on unsteady S vortices. In that case, a meridional propagation speed C_y was also necessary to minimize (8). The results were surprisingly good in the sense that the propagation speed we obtained usually roughly matched the one we calculated from the vortex center trajectory. Also the dispersion (S_c) in the core of the vortex usually decreased after the initial rearrangement took place; it stayed large in the exterior field because of large meridional propagation speed. This seems to prove that S-vortices have a tendency toward homogenization of PV along Ψ contours, at least in the core of the vortex. Thus, we believe that the long time behavior of S-vortices on the β plane is either to reach the rest latitude of the negative pole (the positive pole then has to detach) or a latitude for which both positive and negative poles will have about the same strength, and form a modon. We have, however, been unable until now to find what distinguishes between these two different fates.

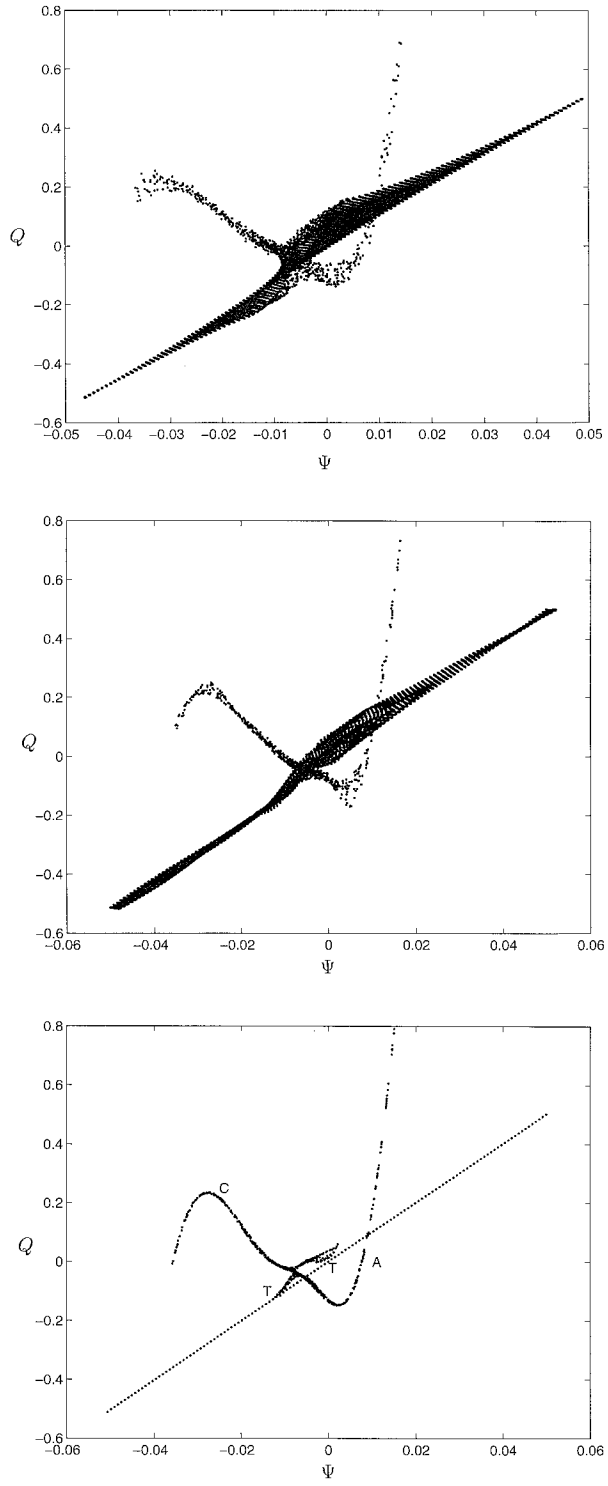

FIG. 11. Evolution of the scatterplot (total PV against the streak function $\Psi = \psi + C_x y$) for the vortex described in the text at 2100 m: (a) initial Q/Ψ relationship, (b) after 100 days, and (c) after 300 days. In order to filter out the remaining traces of Rossby waves in plot (c), we have only represented the scatterplot in the core of the vortex (where the PV anomaly is strong) and superimposed the linear Q/Ψ relationship valid for streaklines extending to infinity (dotted line). Two branches can be distinguished, one corresponding to the anticyclone (**A**) and the other to the cyclone (**C**). Notice the points (**T**) where the nonlinear curves matches with the linear one and which represents the transition between interior and exterior regions.

From PV conservation arguments and analysis of the change in shape of observed meddies, Colin de Verdière (1992) argued that isopycnal mixing on the edge of the vortex could lead to an enhanced southward displacement of meddies on the β plane. As a preliminary study, this hypothesis was tested using the subgrid-scale form of mixing on isopycnal surfaces proposed by Gent and McWilliams (1990) and implemented in a balance model. [The balance equations are intermediate between quasigeostrophic and primitive equations and take into account corrections to QG due to finite Rossby number (V/fL) and small Burger number (NH/fL); see McWilliams and Gent 1980 and Norton et al. 1986.] The solutions yielded two results: 1) moderate mixing does not induce any significant change in the evolution and displacement of vortices on the β plane, at least with the present parameterization; and 2) differences in vortex trajectories between the QG and balance models are generally modest for meddy parameters. Thus, we believe that the absence in the present study of isopycnal mixing and higher-order dynamics do not seriously detract from the relevance of our conclusions.

Isolated S-vortices have significant PV anomalies of both signs, and they must have cyclonic partners above or below the main anticyclonic core. This raises the issue of how close our solutions are to meddies or other submesoscale coherent vortices.

The Burger number of most observed submesoscale coherent structures is small (McWilliams 1985), which implies that the PV anomaly is dominated by stretching in the core anticyclone; furthermore, meddies are distinguished among other submesoscale coherent vortices by having a particularly small Burger number. This has been further confirmed by recent measurements at sea: Pingree and Le Cann (1993b) and Schultz-Tokos and Rossby (1991) have measured the PV associated with a meddy and shown that it was dominated by stretching. It is clear from their work that a positive PV anomaly exists below and probably also above the main core.

The source for a positive PV anomaly is uncertain, but there are reasons to believe that the Mediterranean outflow entrainment, mixing, and subsequent current along the Iberian continental slope might be embedded between layers of positive PV anomaly. A source of positive PV anomaly should arise through the intense isopycnal or diapycnal mixing when Mediterranean waters enter the Atlantic basin (Baringer 1993) since vertical mixing yields weaker stratification in the center and stronger stratification at the edges. Recent experiments in rotating tanks (Baey et al. 1995; Morel 1995a) show that intermediate vortex formation through ver-

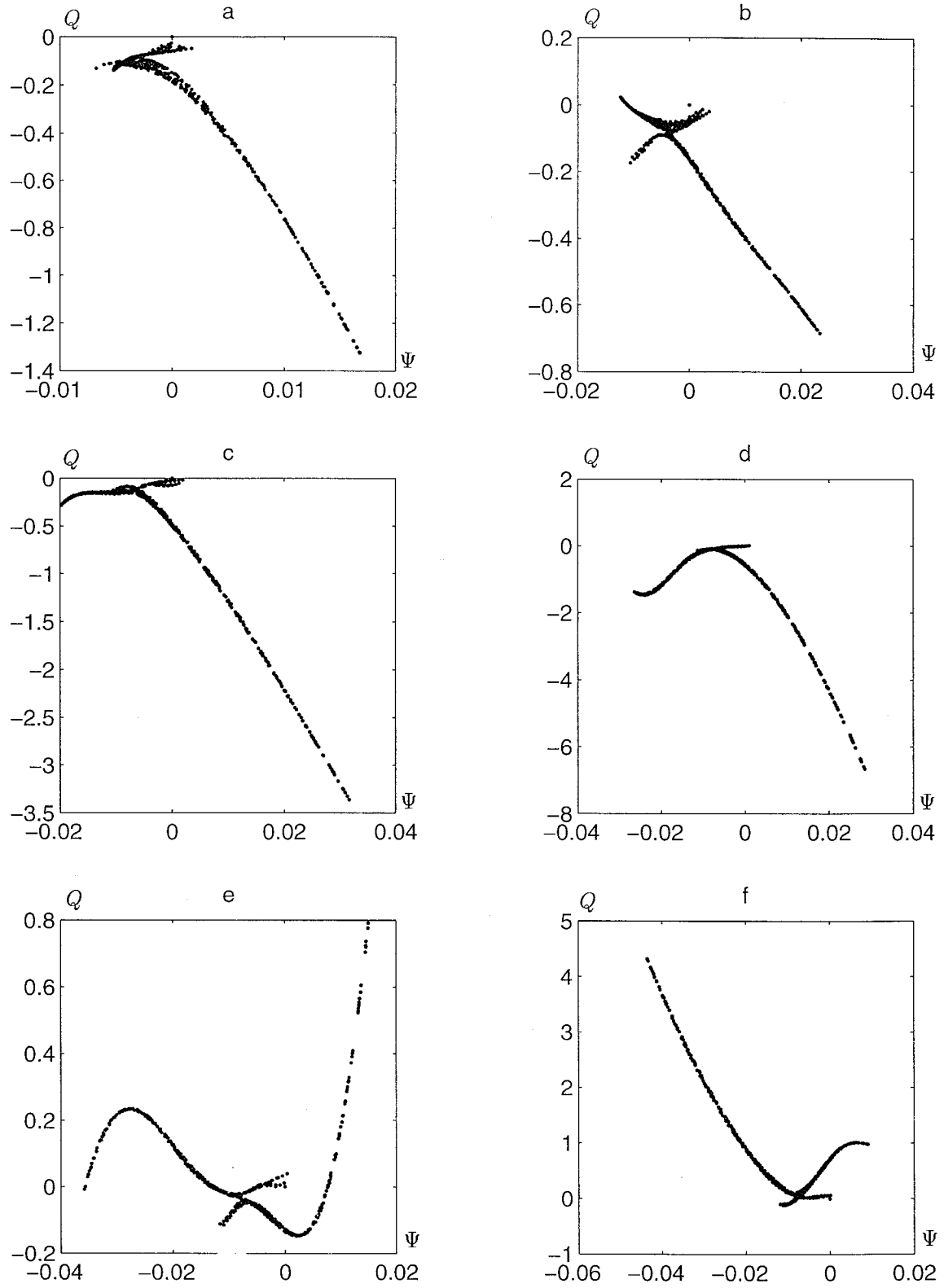

FIG. 12. Scatterplots of the total PV against the streak function ($\Psi = \psi + C_y y$) in the core of the vortex described in the text at (a) 700, (b) 1100, (c) 1500, (d) 1800, (e) 2100, and (f) 2400 m. The scatter is very weak and the Q/Ψ relationships in the core of the vortex are nonlinear. Here the core has been defined as the region where the PV anomaly is strong enough; it includes both cyclonic and anticyclonic regions.

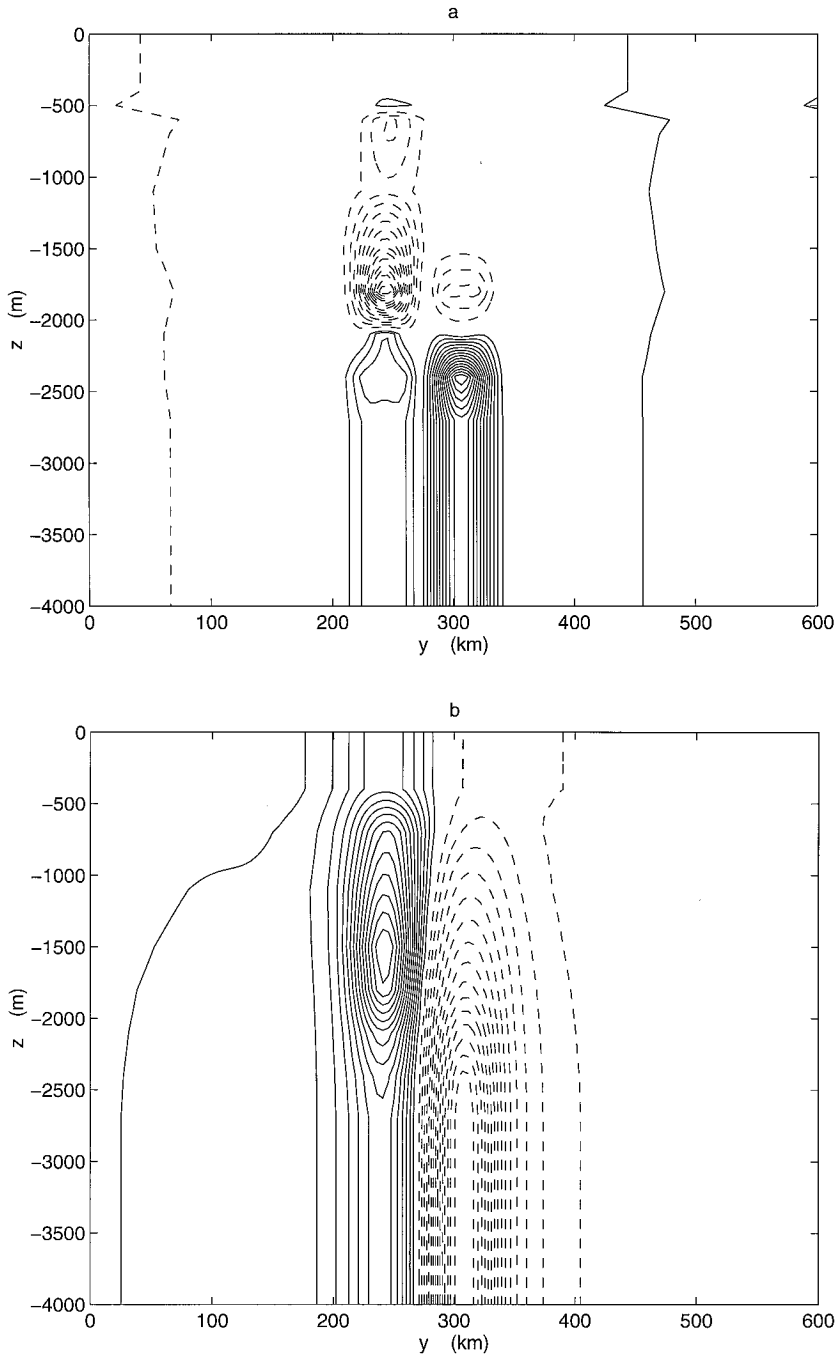

FIG. 13. North–south vertical cross section through the core of the modon described in the text. (a) Total PV and (b) streamfunction.

tical or horizontal injection of intermediate density fluid in a stratified medium generates diapycnal mixing and leads to the creation of a cyclone associated with a positive PV. Also, the meddy formation mechanism through baroclinic instability of the mediterranean current proposed by Prater (1992) requires a change of sign of the gradient of PV at different depths, which is usually associated with opposite sign PV anomalies.

In our numerical solutions, S-vortices develop a strong tendency toward tilting of their vertical axis, which ends up in the formation of one or two cyclonic partners above or below the main core. Most observations of meddies have not indicated a cyclonic companion in the vicinity, but the neighborhood is often poorly surveyed. Pingree and Le Cann (1993a) have observed the evolution of a shallow meddy and showed

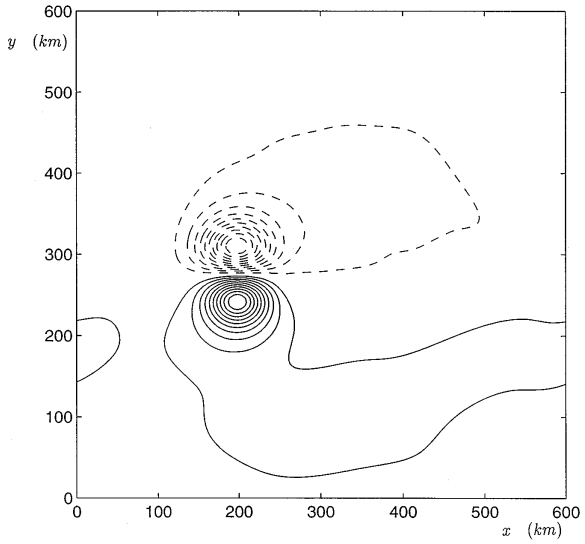

FIG. 14. Barotropic component of the streamfunction associated with the modon described in the text.

that it was initially accompanied by a cyclonic partner in the upper part of the ocean. However, this cyclone seemed to be detached from the main core after about 30 days. More recently a cyclonic circulation has been observed associated with a meddy near the Azores (A. Tychensky 1994, personal communication). This cyclonic feature was again intensified in the upper part of the ocean, and it could have been present from the beginning.

Thus, we believe that meddies, or coherent interior structures in general, could be S-vortices and that the mechanisms described in this paper could explain their trajectories. Clearly, this question must be addressed and more extensive measurements at sea in the vicinity of their cores are required to look for cyclonic companions. If this proves to be a realistic description of a meddy, then this study shows that the observed variety of trajectories and propagation speeds can be due to a hetonic interaction between the opposite-sign PV poles. Up to now, no other mechanism has yielded results as close to observations.

Acknowledgments. We wish to particularly thank Alain Colin de Verdière and Nancy Norton for participating in earlier experiments with the balance model that helped identify the issues addressed here, and Dr. Xavier Carton for his advice and comments. This research was supported by the National Center for Atmospheric Research, which is sponsored by the National Science Foundation and the French Navy Hydrographic and Oceanographic Service.

REFERENCES

Armi, L., 1989: Two years in the life of a Mediterranean salt lens. *J. Phys. Oceanogr.,* **19,** 354–370.

Baey, J. M., D. Renouard, and G. Chabert d'Hières, 1995: Preliminary results about the stability of an intermediate water current. *Deep-Sea Res.,* **42,** 2063–2074.

Baringer, M. O., 1993: Mixing and dynamics of the Mediterranean outflow. Ph.D. thesis, MIT/WHOI, WHOI-93-52, 240 pp.

Beckmann, A., and R. Käse, 1989: Numerical simulation of the movement of a Mediterranean water lens. *Geophys. Res. Lett.,* **16**(1), 65–68.

Berestov, A., 1981: Some new solutions for the Rossby solitons. *Izv. Acad. Sci. USSR, Atmos. Oceanic Phys.,* **17,** 60–64.

Carton, X., and J. McWilliams, 1989: Barotropic and baroclinic instabilities of axisymmetric vortices in a quasigeostrophic model. Mesoscale, synoptic coherent structures in geophysical turbulence. *Proc. 20th Int. Liège Colloq. on Ocean Hydrodynamics,* J. C. J. Nihoul and B. M. Jamart, Eds., Oceanography Series, Vol. 50, Elsevier, 225–244.

——, and ——, 1996: Nonlinear oscillatory evolution of a baroclinically unstable geostrophic vortex. *Dyn. Atmos. Oceans,* **24,** 207–214.

Chérubin, L., X. Carton, and D. Dritschel, 1995: Vortex expulsion by a zonal coastal jet on a transverse canyon. *Proc. 2d IWVF Meeting in Montreal,* Montreal, Quebec, Canada, ESAIM, 101–121.

Colin de Verdière, A., 1992: On the southward motion of Mediterranean salt lenses. *J. Phys. Oceanogr.,* **22,** 413–420.

Dewar, W., and H. Meng, 1995: The propagation of submesoscale coherent vortices. *J. Phys. Oceanogr,* **25,** 1745–1770.

Flierl, G. R., 1987: Isolated eddy models in geophysics. *Annu. Rev. Fluid Mech.,* **19,** 493–530.

——, 1988: On the instability of geostrophic vortices. *J. Fluid Mech.,* **197,** 349–388.

——, V. D. Larichev, J. C. McWilliams, and G. M. Reznik, 1980: The dynamics of baroclinic and barotropic solitary eddies. *Dyn. Atmos. Oceans,* **5,** 1–41.

—— M. E. Stern, and J. A. Whitehead, 1983: The physical significance of modons: Laboratory experiments and general integral constraints. *Dyn. Atmos. Oceans,* **7,** 233–263.

Gent, P., and J. McWilliams, 1986: The instability of barotropic circular vortices. *Geophys. Astrophys. Fluid Dyn.,* **35**(3), 209–233.

——, and ——, 1990: Isopycnal mixing in ocean circulation models. *J. Phys. Oceanogr,* **20,** 150–155.

Hogg, N. G., and H. M. Stommel, 1985: The heton, an elementary interaction between discrete baroclinic geostrophic vortices, and its implications concerning eddy heat flow. *Proc. Roy. Soc. London, Ser. A,* **397,** 1–20.

——, and ——, 1990: How current in the upper thermocline could advect meddies deeper down. *Deep-Sea Res.,* **37**(4), 613–623.

Kizner, Z., 1983: Rossby solitons with axisymmetric baroclinic modes. *Dokl. Akad., Nauk SSSR,* **275**(6), 1495–1498.

Madelain, F., 1970: Influence de la topographie du fond sur l'écoulement Méditerranéen entre le détroit de Gibraltar et le cap Saint Vincent. *Cah. Océanogr.,* **22,** 44–61.

McWilliams, J. C., 1985: Submesoscale, coherent vortices in the ocean. *Rev. Geophys.,* **23**(2), 165–182.

——, and G. R. Flierl, 1979: On the evolution of isolated, nonlinear vortices. *J. Phys. Oceanogr.,* **9,** 1155–1182.

——, and P. Gent, 1980: Intermediate models of planetary circulations in the atmosphere and ocean. *J. Atmos. Sci.,* **37,** 1657–1678.

——, W. R. Holland, and J. H. S. Chow, 1978: A description of numerical Antarctic circumpolar current. *Dyn. Atmos. Oceans,* **2,** 213–291.

——, P. Gent, and N. Norton, 1986: The evolution of balanced, low mode vortices on the beta plane. *J. Phys. Oceanogr.,* **16,** 838–855.

——, N. Norton, P. Gent, and D. Haidvogel, 1990: A linear balance model of wind-driven, midlatitude ocean circulation. *J. Phys. Oceanogr.,* **20,** 1349–1378.

Mied, R. P., and G. J. Lindemann, 1982: The birth and evolution of eastward-propagating modons. *J. Phys. Oceanogr.,* **12,** 213–230.

Morel, Y., 1995a: Etude des déplacements et de la dynamique des

tourbillons géophysiques. Application aux Meddies. These de doctorat, l'Université Joseph Fourier, 155 pp. [Available from Université Joseph Fourier, BP 53X, 38041 Grenoble Cedex, France.]

——, 1995b: The effect of an upper-thermocline current on intra-thermocline eddies. *J. Phys. Oceanogr.,* **25,** 3247–3252.

——, and X. Carton, 1994: Multipolar vortices in two-dimensional incompressible flows. *J. Fluid Mech.,* **267,** 23–51.

Norton, N., J. McWilliams, and P. Gent, 1986: A numerical model of the balance equations in a periodic domain and an example of balanced turbulence. *J. Comput. Phys.,* **67,** 439–471.

Olson, D. B., 1980: The physical oceanography of two rings observed by the cyclonic ring experiment. Part II: Dynamics. *J. Phys. Oceanogr.,* **10,** 514–528.

Orszag, 1971: Numerical simulation of incompressible flows within simple boundaries. I. Galerkin (spectral) representations. *Stud. Appl. Math.,* 293–328.

Pakyari, A. R., and J. Nycander, 1996: Steady two-layer vortices on the beta-plane. *Dyn. Atmos. Oceans,* in press.

Pedlosky, J., 1987: *Geophysical Fluid Dynamics.* Springer, 710 pp.

Pichevin, T., and D. Nof, 1995: The eddy canon. *Deep-Sea Res.,* **43,** 1475–1507.

Pingree, R. D., and B. Le Cann, 1993a: A shallow meddy (a smeddy) from the secondary Mediterranean salinity maximum. *J. Geophys. Res.,* **98,** 20 169–20 185.

——, and ——, 1993b: Structure of a meddy (Bobby 92) southeast of the Azores. *Deep-Sea Res.,* **40,** 2077–2103.

Prater, M., 1992: Observation and hypothesized generation of a meddy in the Gulf of Cadiz. Ph.D. dissertation, UW TR9210, Applied Physics Laboratory, University of Washington, 131 pp.

——, and T. Sanford, 1994: A meddy off Cape St. Vincent. Part I: Description. *J. Phys. Oceanogr.,* **24,** 1572–1586.

Rayleigh, L., 1880: On the stability, or instability, of certain fluid motions. *Proc. London Math. Soc.,* **11,** 57–70.

Richardson, P. L., D. Walsh, L. Armi, M. Schroder, and J. F. Price, 1989: Tracking three meddies with SOFAR floats. *J. Phys. Oceanogr.,* **19,** 371–383.

——, M. S. McCartney, and C. Maillard, 1991: A search for meddies in historical data. *Dyn. Atmos. Oceans,* **15,** 241–265.

Schultz-Tokos, K., and T. Rossby, 1991: Kinematics and dynamics of a Mediterranean salt lens. *J. Phys. Oceanogr.,* **21,** 879–892.

Stern, M., 1975: Minimal properties of planetary eddies. *J. Mar. Res.,* **33,** 1–13.

Sutyrin, G. G., and G. R. Flierl, 1994: Intense vortex motion on the beta plane: Development of the beta gyres. *J. Atmos. Sci.,* **51,** 773–790.

Swenson, M., 1987: Instability of equivalent-barotropic riders. *J. Phys. Oceanogr.,* **17,** 492–506.

Tychensky, A., 1994: Traitement et analyse des données de la campagne SEMAPHORE. Application à la caractérisation hydrologique et dynamique des meddies observés pendant cette campagne. Rapport de Stage de DEA, 150 pp. [Available from EP-SHOM-CMO, BP 426, 29275, Brest Cedex, France.]

Zenk, W., and L. Armi, 1990: The complex spreading pattern of Mediterranean water off the Portuguese continental shelf. *Deep-Sea Res.,* **37,** 1805–1823.